# Supplementary Material

## Small-Angle X-ray Scattering Unveils the Internal Structure of Lipid Nanoparticles

Francesco Spinozzi[a*], Paolo Moretti[a], Diego Romano Perinelli[b], Giacomo Corucci[c], Paolo Piergiovanni[a], Heinz Amenitsch[d], Giulio Alfredo Sancini[e], Giancarlo Franzese[f], Paolo Blasi[g*]

[a] Department of Life and Environmental Sciences, Polytechnic University of Marche, Italy

[b] School of Pharmacy, University of Camerino, Camerino, Italy

[c] Institut Laue-Langevin, Grenoble, France and École Doctorale de Physique, Université Grenoble Alpes, Saint-Martin-d'Héres, France and Department of Chemistry, Imperial College London, London, UK

[d] Institute for Inorganic Chemistry, Graz University of Technology, Graz, Austria

[e] School of Medicine and Surgery, University of Milan Bicocca, Milan, Italy

[f] Secció de Física Estadística i Interdisciplinària - Departament de Física de la Matèria Condensada, & Institut de Nanociència i Nanotecnologia, Universitat de Barcelona, Martí i Franquès 1, Barcelona, 08028, Spain

[g] Department of Pharmacy and Biotechnology, University of Bologna, Bologna, Italy

## S1  Analysis of DLS measurements

According to Siegert's relationship, the second-order auto-correlation function of the light intensity measured by a DLS experiment for a suspension of monodisperse particles is

$$g_2(\tau) - 1 = e^{-2Dq^2\tau}, \tag{S1}$$

where $q = (4\pi/\lambda)n_0 \sin(\theta/2)$ is the modulus of light scattering vector, $\lambda$, $n_0$ and $\theta$ being the light wavelength, the solvent refraction index, and the scattering angle, respectively. By assuming a Brownian motion of the particles caused by the movement of solvent molecules that surround them, the translational diffusion coefficient, $D$, can be approximated by the Stokes-Einstein equation,

$$D = \frac{k_B T}{6\eta R_H} \tag{S2}$$

where $k_B$ is Boltzmann's constant, $T$ the absolute temperature, $\eta$ the viscosity of the solvent at $T$ and $R_H$ is the radius of sphere that best approximates the hydrated particle shape (hydrodynamic radius). In the case of particles with polydisperse dimensions and assuming a simple Gaussian distribution function of $R_H$, the auto-correlation function becomes

$$g_2(\tau) - 1 = \int_{R_{H,\mathrm{lb}}}^{R_{H,\mathrm{ub}}} e^{-2Dq^2\tau} p(R_H) dR_H \tag{S3}$$

where

$$p(R_H) = \frac{1}{Z_{R_H}} e^{-(R_H - R_{H,\mathrm{max}})^2/(2\xi_{R_{H,\mathrm{max}}}^2 R_{H,\mathrm{max}}^2)} \tag{S4}$$

In this equation, $R_{H,\mathrm{lb}} = \max\{R_{H,\mathrm{max}}(1 - p_G\xi_{R_{H,\mathrm{max}}}), R_{H,\mathrm{min}}\}$ and $R_{H,\mathrm{ub}} = R_{H,\mathrm{max}}(1 + p_G\xi_{R_{H,\mathrm{max}}})$ are the lower and the upper bounds of the integrals calculated on the basis of the dispersion $\xi_{R_{H,\mathrm{max}}}$. Notice that in these equations, $R_{H,\mathrm{min}}$ is the minimum allowed value of the lower integration bound, which cannot be negative. In our case we fixed $R_{H,\mathrm{min}} = 50$ Å. The normalization factor $Z_{R_H}$ is determined by the following equation

$$
\begin{aligned}
Z_{R_H} &= \int_{R_{H,\mathrm{lb}}}^{R_{H,\mathrm{ub}}} e^{-(R_H - R_{H,\mathrm{max}})^2/(2\xi_{R_{H,\mathrm{max}}}^2 R_{H,\mathrm{max}}^2)} dR_H \\
&= (\sqrt{2\pi}(\mathrm{erf}((R_{H,\mathrm{ub}} - R_{H,\mathrm{max}})/(\sqrt{2}\xi_{R_{H,\mathrm{max}}} R_{H,\mathrm{max}}))) \\
&\quad - \mathrm{erf}((R_{H,\mathrm{lb}} - R_{H,\mathrm{max}})/(\sqrt{2}\xi_{R_{H,\mathrm{max}}} R_{H,\mathrm{max}})))/2.
\end{aligned}
\tag{S5}
$$

The integral in Eq. S3 is numerically calculated with Simpson's rule by using 100 points. The average of the $k$-power of the hydration radius is defined as

$$<R_H^k> = \frac{1}{Z_{R_H}} \int_{R_{H,\mathrm{lb}}}^{R_{H,\mathrm{ub}}} R_H^k e^{-(R_H - R_{H,\mathrm{max}})^2/(2\xi_{R_{H,\mathrm{max}}}^2 R_{H,\mathrm{max}}^2)} dR_H \tag{S6}$$

The average hydration radius, corresponding to $k = 1$ in Eq. S6, is

$$
\begin{aligned}
<R_H> \quad = \quad & -\exp(-R_{H,\text{max}}^2/s^2 - R_{H,\text{ub}}^2/s^2 - R_{H,\text{lb}}^2/s^2)(s^2 \exp(R_{H,\text{ub}}^2/s^2 \\
& + (2R_{H,\text{max}}R_{H,\text{lb}})/s^2) - s^2 \exp((2R_{H,\text{max}}R_{H,\text{ub}})/s^2 + R_{H,\text{lb}}^2/s^2) \\
& -\sqrt{\pi}sR_{H,\text{max}}\text{erfc}((R_{H,\text{ub}} - R_{H,\text{max}})/s)\exp(R_{H,\text{max}}^2/s^2 \\
& + R_{H,\text{ub}}^2/s^2 + R_{H,\text{lb}}^2/s^2) \\
& + \sqrt{\pi}sR_{H,\text{max}}\exp(R_{H,\text{max}}^2/s^2 + R_{H,\text{ub}}^2/s^2 \\
& + R_{H,\text{lb}}^2/s^2)\text{erfc}((R_{H,\text{lb}} - R_{H,\text{max}})/s))/\sqrt{\pi}.
\end{aligned}
\tag{S7}
$$

where $s^2 = 2R_{H,\text{max}}^2\xi_{R_{H,\text{max}}}^2$. The second moment of the distribution is the case $k = 2$, which reads

$$
\begin{aligned}
<R_H^2> \quad = \quad & -\exp(-R_{H,\text{max}}^2/s^2 - R_{H,\text{ub}}^2/s^2 - R_{H,\text{lb}}^2/s^2)(2s^2 R_{H,\text{max}} \exp(R_{H,\text{ub}}^2/s^2 \\
& + (2R_{H,\text{max}}R_{H,\text{lb}})/s^2) + 2s^2 R_{H,\text{lb}} \exp(R_{H,\text{ub}}^2/s^2 \\
& + (2R_{H,\text{max}}R_{H,\text{lb}})/s^2) - 2s^2 R_{H,\text{max}} \exp((2R_{H,\text{max}}R_{H,\text{ub}})/s^2 \\
& + R_{H,\text{lb}}^2/s^2) - 2s^2 R_{H,\text{ub}} \exp((2R_{H,\text{max}}R_{H,\text{ub}})/s^2 + R_{H,\text{lb}}^2/s^2) \\
& -\sqrt{\pi}s^3\text{erfc}((R_{H,\text{ub}} - R_{H,\text{max}})/s)\exp(R_{H,\text{max}}^2/s^2 \\
& + R_{H,\text{ub}}^2/s^2 + R_{H,\text{lb}}^2/s^2) \\
& -2\sqrt{\pi}sR_{H,\text{max}}^2\text{erfc}((R_{H,\text{ub}} - R_{H,\text{max}})/s)\exp(R_{H,\text{max}}^2/s^2 \\
& + R_{H,\text{ub}}^2/s^2 + R_{H,\text{lb}}^2/s^2) + \sqrt{\pi}s^3 \exp(R_{H,\text{max}}^2/s^2 + R_{H,\text{ub}}^2/s^2 \\
& + R_{H,\text{lb}}^2/s^2)\text{erfc}((R_{H,\text{lb}} - R_{H,\text{max}})/s) \\
& + 2\sqrt{\pi}sR_{H,\text{max}}^2 \exp(R_{H,\text{max}}^2/s^2 + R_{H,\text{ub}}^2/s^2 \\
& + R_{H,\text{lb}}^2/s^2)\text{erfc}((R_{H,\text{lb}} - R_{H,\text{max}})/s))/2.
\end{aligned}
\tag{S8}
$$

The dispersion of $R_H$ is calculated as

$$
\xi_{R_H} = (<R_H^2> / <R_H>^2 - 1)^{1/2}.
\tag{S9}
$$

# S2    Average micelle aggregation number

$$
\begin{aligned}
<m> \quad = \quad & \frac{z}{C_{\text{P80}}} e^{\delta/(RT)} \\
& + e^{-(\Delta - m_0 \delta)/(RT)} z^{m_0} \frac{z^2(m_0-1)^2 + z[1 - 2m_0(m_0-1)] + m_0^2}{C_{\text{P80}}(1-z)^3}
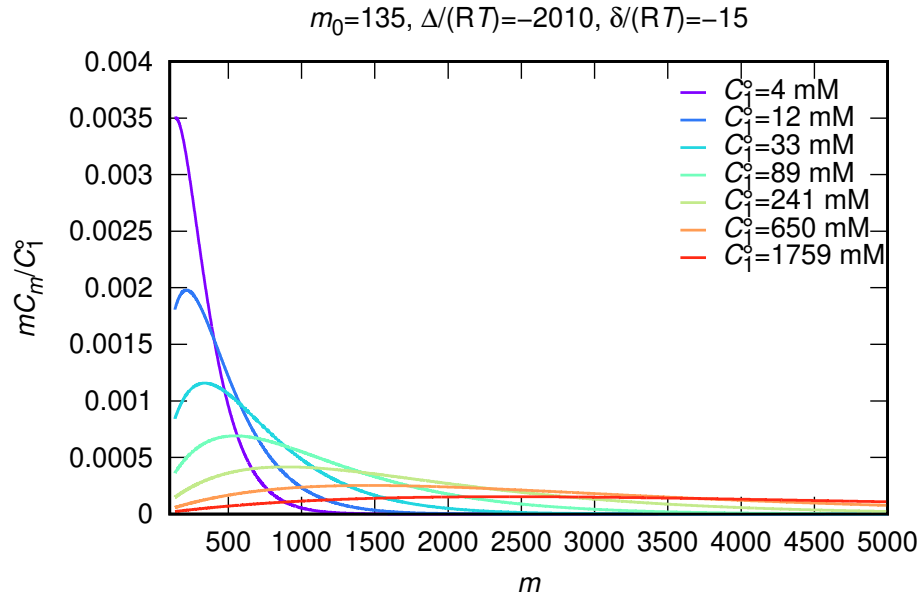\end{aligned}
\tag{S10}
$$



Figure S1: Size distribution of a cylinder with spherical end-caps according to the ladder model

# S3 SAXS amplitude of the core-shell end-cap cylinder

The SAXS amplitude of the core-shell end-cap cylinder formed by $m$ P80 molecules reads[1]

$$A_{\text{ec},m}(\mathbf{q}) = G \sin\left(q_{\parallel} B(m - m_0)\right) + F \cos\left(q_{\parallel} B(m - m_0)\right) \tag{S11}$$

$$G = \sum_{k=1}^{2} \frac{4\pi}{q_{\parallel}} (\rho_{k,\text{cyl}} - \rho_{k-1,\text{cyl}}) R_{k,\text{cyl}}^2 \frac{J_1(q_{\perp} R_{k,\text{cyl}})}{q_{\perp} R_{k,\text{cyl}}}$$

$$- \sum_{k=1}^{2} \int_{-h/R_{k,\text{cap}}}^{1} dX\, H_k(X) \sin(q_{\parallel}[X\,R_{k,\text{cap}} + h]) \tag{S12}$$

$$B = \frac{\nu_{\text{hyd,cyl}}}{2\pi R_{2,\text{cyl}}^2} \tag{S13}$$

$$F = \sum_{k=1}^{2} \int_{-h/R_{k,\text{cap}}}^{1} dX\, H_k(X) \cos(q_{\parallel}[X\,R_{k,\text{cap}} + h]) \tag{S14}$$

$$H_k(X) = 4\pi R_{k,\text{cap}}^3 (\rho_{k,\text{cap}} - \rho_{k-1,\text{cap}})(1 - X^2) \frac{J_1(q_{\perp} R_{k,\text{cap}}\sqrt{1 - X^2})}{q_{\perp} R_{k,\text{cap}}\sqrt{1 - X^2}} \tag{S15}$$

where $J_1(x)$ is the Bessel functions of the first order, $R_{1,\text{cyl}} = R_{2,\text{cyl}} + \delta_{\text{cyl}}$ and $R_{1,\text{cap}} = R_{2,\text{cap}} + \delta_{\text{cap}}$. Moreover, $\rho_{0,\text{cyl}} \equiv \rho_{0,\text{cap}} \equiv \rho_0$ is the ED of bulk water.

The corresponding orientational average squared amplitude (the so-called form factor) and the average amplitude of the $m$-micelle are the following integrals

$$P_{\text{ec},m}(q) = \int_0^{\pi/2} d\beta_q \sin\beta_q A_{\text{ec},m}^2(\mathbf{q}) \tag{S16}$$

$$P_{\text{ec},m}^{(1)}(q) = \int_0^{\pi/2} d\beta_q \sin\beta_q A_{\text{ec},m}(\mathbf{q}) \tag{S17}$$

The numerical calculus of these integrals is realized with the 32-point Gauss-Legendre quadrature method. The working factors appearing in Eqs. 8 and 9 are:

$$N_2 = 2q_{\parallel}^2 B^2 (F^2 + G^2) + EF(EF + 2q_{\parallel} BG) \tag{S18}$$

$$D_2 = E^2 + 4q_{\parallel}^2 B^2 \tag{S19}$$

$$N_1 = E(EF + q_{\parallel} BG) \tag{S20}$$

$$D_1 = E^2 + q_{\parallel}^2 B^2 \tag{S21}$$

All the electron densities are calculated based on the volumetric properties of each group forming the P80 molecule and considering the number of water molecules embedded among the polar heads
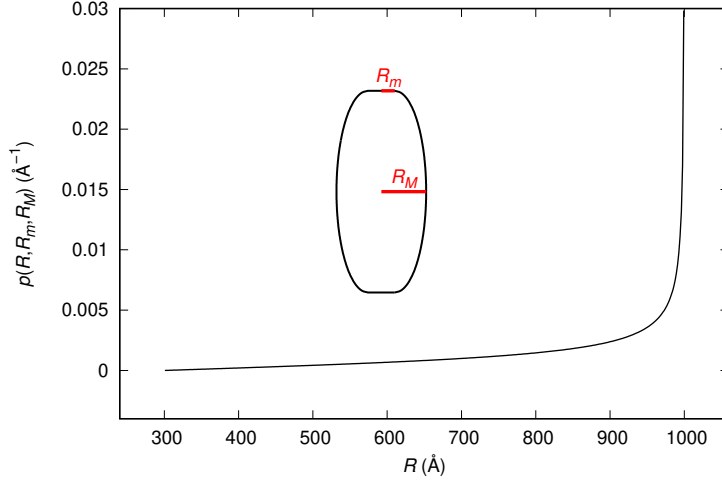
Figure S2: Distribution function of the circular cross-section radius of a barrel with an elliptical radial profile (Eq. 11). Parameters are $R_m = 300$ Å and $R_M = 1000$ Å.

in the $k = 1$ domain of both the end-cap and the cylinder regions. Detailed expressions are reported in the Sect. S11.2 (Eqs. S65, S68, S69, S70, S71 and S72).

# S4 Distribution function of the circular cross-section radius of a polydisperse barrel shape with smooth radial elliptical profile

The normalization factor $Z_{R_M}$, seen in Eq. 13, is given by

$$
\begin{aligned}
Z_{R_M} &= \int_{R_{M,\mathrm{lb}}}^{R_{M,\mathrm{ub}}} e^{-(R_M - R_{M,\max})^2/(2\xi_{R_M}^2 R_{M,\max}^2)} dR_M \\
&= (\sqrt{2\pi}(\mathrm{erf}((R_{M,\mathrm{ub}} - R_{M,\max})/(\sqrt{2}\xi_{R_M} R_{M,\max}))) \\
&\quad - \mathrm{erf}((R_{M,\mathrm{lb}} - R_{M,\max})/(\sqrt{2}\xi_{R_M} R_{M,\max})))/2.
\end{aligned}
\tag{S22}
$$

The average platelet radius and its dispersion, defined in Eqs. 14-15, are

$$
R_0 = G_1/Z_{R_M}((4 - \pi)\nu + \pi)/4
\tag{S23}
$$

$$
\xi_R = \sqrt{<R^2>/R_0^2 - 1}
\tag{S24}
$$

$$
<R^2> = G_2/Z_{R_M}((10 - 3\pi)\nu^2 + (3\pi - 8)\nu + 4)/6
\tag{S25}
$$

where

$$
\begin{aligned}
G_1 \;=\; & ((\xi_{R_M} R_{M,\mathrm{max}}) \exp((-(R_{M,\mathrm{lb}}^2/(\xi_{R_M} R_{M,\mathrm{max}})^2)/2) \\
& -(R_{M,\mathrm{ub}}^2/(\xi_{R_M} R_{M,\mathrm{max}})^2)/2 - (R_{M,\mathrm{max}}^2/(\xi_{R_M} R_{M,\mathrm{max}})^2)/2)(2(\xi_{R_M} R_{M,\mathrm{max}}) \\
& \exp((R_{M,\mathrm{max}} R_{M,\mathrm{lb}})/(\xi_{R_M} R_{M,\mathrm{max}})^2 + (R_{M,\mathrm{ub}}^2/(\xi_{R_M} R_{M,\mathrm{max}})^2)/2) \\
& -2(\xi_{R_M} R_{M,\mathrm{max}}) \exp((R_{M,\mathrm{lb}}^2/(\xi_{R_M} R_{M,\mathrm{max}})^2)/2 + ( \\
& R_{M,\mathrm{max}} R_{M,\mathrm{ub}})/(\xi_{R_M} R_{M,\mathrm{max}})^2) - \sqrt{2}\sqrt{\pi} R_{M,\mathrm{max}} \mathrm{erfc}((R_{M,\mathrm{ub}} - R_{M,\mathrm{max}})/(\sqrt{2} \\
& (\xi_{R_M} R_{M,\mathrm{max}}))) \exp((R_{M,\mathrm{lb}}^2/(\xi_{R_M} R_{M,\mathrm{max}})^2)/2 + (R_{M,\mathrm{ub}}^2/(\xi_{R_M} R_{M,\mathrm{max}})^2)/2 \\
& +(R_{M,\mathrm{max}}^2/(\xi_{R_M} R_{M,\mathrm{max}})^2)/2) + \sqrt{2}\sqrt{\pi} \\
& R_{M,\mathrm{max}} \mathrm{erfc}((R_{M,\mathrm{lb}} - R_{M,\mathrm{max}})/(\sqrt{2}(\xi_{R_M} R_{M,\mathrm{max}}))) \\
& \exp((R_{M,\mathrm{lb}}^2/(\xi_{R_M} R_{M,\mathrm{max}})^2)/2 + (R_{M,\mathrm{ub}}^2/ \\
& (\xi_{R_M} R_{M,\mathrm{max}})^2)/2 + (R_{M,\mathrm{max}}^2/(\xi_{R_M} R_{M,\mathrm{max}})^2)/2)))/2 \qquad \text{(S26)}
\end{aligned}
$$

$$
\begin{aligned}
G_2 \;=\;\; & ((\xi_{R_M} R_{M,\max}) \exp((-(R_{M,\text{lb}}^2/(\xi_{R_M} R_{M,\max})^2)/2) \\
& -(R_{M,\text{ub}}^2(\xi_{R_M} R_{M,\max})^2)/2 - (R_{M,\max}^2/(\xi_{R_M} R_{M,\max})^2)/2)(2R_{M,\max} \\
& (\xi_{R_M} R_{M,\max}) \exp((R_{M,\max} R_{M,\text{lb}})/(\xi_{R_M} R_{M,\max})^2 \\
& +(R_{M,\text{ub}}^2/(\xi_{R_M} R_{M,\max})^2)) + 2R_{M,\text{lb}}(\xi_{R_M} R_{M,\max}) \exp(( \\
& R_{M,\max} R_{M,\text{lb}})/(\xi_{R_M} R_{M,\max})^2 + (R_{M,\text{ub}}^2/(\xi_{R_M} R_{M,\max})^2)/2) \\
& -2R_{M,\max}(\xi_{R_M} R_{M,\max}) \exp((R_{M,\text{lb}}^2(\xi_{R_M} R_{M,\max})^2)/2 + ( \\
& R_{M,\max} R_{M,\text{ub}})/(\xi_{R_M} R_{M,\max})^2) - 2R_{M,\text{ub}}(\xi_{R_M} R_{M,\max}) \\
& \exp((R_{M,\text{lb}}^2/(\xi_{R_M} R_{M,\max})^2)/2 + (R_{M,\max} R_{M,\text{ub}})(\xi_{R_M} R_{M,\max})^2) - \\
& \sqrt{2}\sqrt{\pi} R_{M,\max}^2 \mathrm{erfc}((R_{M,\text{ub}} - R_{M,\max})/(\sqrt{2}(\xi_{R_M} R_{M,\max}))) \\
& \exp((R_{M,\text{lb}}^2/ \\
& (\xi_{R_M} R_{M,\max})^2)/2 + (R_{M,\text{ub}}^2(\xi_{R_M} R_{M,\max})^2)/2 + (R_{M,\max}^2/(\xi_{R_M} R_{M,\max})^2)/2) \\
& +\sqrt{2}\sqrt{\pi} R_{M,\max}^2 \mathrm{erfc}((R_{M,\text{lb}} - \\
& R_{M,\max})/(\sqrt{2}(\xi_{R_M} R_{M,\max}))) \exp((R_{M,\text{lb}}^2(\xi_{R_M} R_{M,\max})^2)/2 \\
& +(R_{M,\text{ub}}^2/(\xi_{R_M} R_{M,\max})^2)/2 + (R_{M,\max}^2(\xi_{R_M} R_{M,\max})^2)/2) - \\
& \sqrt{2}\sqrt{\pi} \mathrm{erfc}((R_{M,\text{ub}} - R_{M,\max})/(\sqrt{2}(\xi_{R_M} R_{M,\max})))(\xi_{R_M} R_{M,\max})^2 \exp((R_{M,\text{lb}}^2/ \\
& (\xi_{R_M} R_{M,\max})^2)/2 R_{M,\text{ub}}^2/(\xi_{R_M} R_{M,\max})^2)/2 + (R_{M,\max}^2/(\xi_{R_M} R_{M,\max})^2)/2) \\
& \sqrt{2}\sqrt{\pi} \mathrm{erfc}((R_{M,\text{lb}} - R_{M,\max})/(\sqrt{2} \\
& (\xi_{R_M} R_{M,\max})))(\xi_{R_M} R_{M,\max})^2 \exp((R_{M,\text{lb}}^2/(\xi_{R_M} R_{M,\max})^2)/2 \\
& +(R_{M,\text{ub}}^2/(\xi_{R_M} R_{M,\max})^2)/2 + (R_{M,\max}^2/(\xi_{R_M} R_{M,\max})^2)/2)))/2 
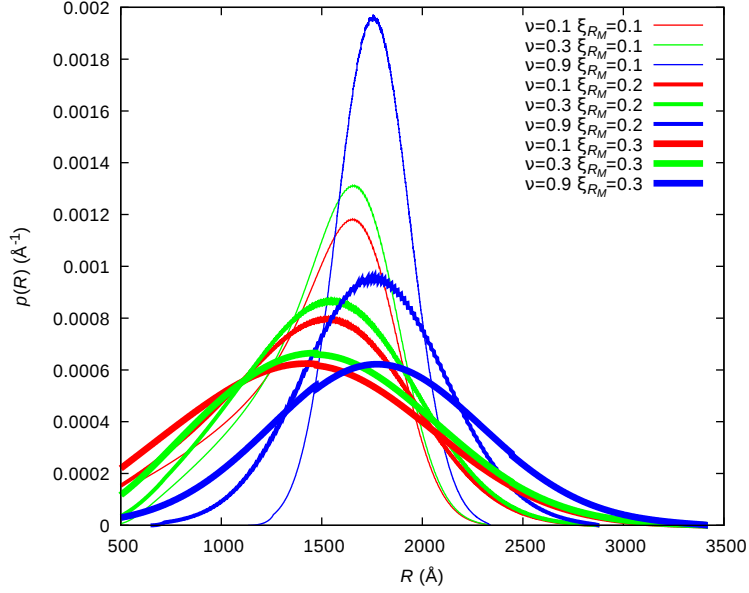\end{aligned} \tag{S27}
$$

Figure S3: $p(R)$ of the circular cross-section radius of a polydisperse barrel shape. $R_{M,\text{max}} = 1800$ Å, $R_{M,\text{min}} = 500$ Å, $p_G = 3$.

## S5 Averages of the half thickness of the core of the platelet and its square over a Gaussian distribution comprised between two bounds

The distribution function of $t$ (the half thickness of the core of the platelet) is

$$p_t(t) = \frac{1}{Z_t} e^{-(t-t_{\text{max}})^2/(2\xi_{t_{\text{max}}}^2 t_{\text{max}}^2)} \tag{S28}$$

The normalization factor $Z_t$ is determined by the following equation

$$
\begin{aligned}
Z_t &= \int_{t_{\text{lb}}}^{t_{\text{ub}}} e^{-(t-t_{\text{max}})^2/(2\xi_{t_{\text{max}}}^2 t_{\text{max}}^2)} dt \\
&= (\sqrt{2\pi}(\text{erf}((t_{\text{ub}} - t_{\text{max}})/(\sqrt{2}\xi_{t_{\text{max}}} t_{\text{max}}))) - \text{erf}((t_{\text{lb}} - t_{\text{max}})/(\sqrt{2}\xi_{t_{\text{max}}} t_{\text{max}})))/2. \tag{S29}
\end{aligned}
$$

where $t_{\text{lb}} = \max\{t_{\text{max}}(1 - p_G\xi_{t_{\text{max}}}), t_{\text{min}}\}$ and $t_{\text{ub}} = t_{\text{max}}(1 + p_G\xi_{t_{\text{max}}})$ are the lower and the upper bounds of the integrals calculated based on the dispersion $\xi_{t_{\text{max}}}$. In these equations, $t_{\text{min}}$ is the minimum allowed value of the lower integration bound, which cannot be negative. In our case we fixed $t_{\text{min}} = 1$ Å.

The average of the $k$-power of the half thickness of the platelet core is defined as

$$<t^k>= \frac{1}{Z_t} \int_{t_{\mathrm{lb}}}^{t_{\mathrm{ub}}} t^k e^{-(t-t_{\mathrm{max}})^2/(2\xi_{t_{\mathrm{max}}}^2 t_{\mathrm{max}}^2)} dt \qquad (S30)$$

The average thickness, corresponding to $k = 1$ in Eq. S30, is

$$
\begin{aligned}
t_0 &= -\exp(-t_{\mathrm{max}}^2/s^2 - t_{\mathrm{ub}}^2/s^2 - t_{\mathrm{lb}}^2/s^2)(s^2\exp(t_{\mathrm{ub}}^2/s^2 \\
&\quad +(2t_{\mathrm{max}}t_{\mathrm{lb}})/s^2) - s^2\exp((2t_{\mathrm{max}}t_{\mathrm{ub}})/s^2 + t_{\mathrm{lb}}^2/s^2) \\
&\quad -\sqrt{\pi}st_{\mathrm{max}}\mathrm{erfc}((t_{\mathrm{ub}} - t_{\mathrm{max}})/s)\exp(t_{\mathrm{max}}^2/s^2 \\
&\quad +t_{\mathrm{ub}}^2/s^2 + t_{\mathrm{lb}}^2/s^2) \\
&\quad +\sqrt{\pi}st_{\mathrm{max}}\exp(t_{\mathrm{max}}^2/s^2 + t_{\mathrm{ub}}^2/s^2 \\
&\quad +t_{\mathrm{lb}}^2/s^2)\mathrm{erfc}((t_{\mathrm{lb}} - t_{\mathrm{max}})/s))/\sqrt{\pi}.
\end{aligned}
\qquad (S31)
$$

where $s^2 = 2t_{\mathrm{max}}^2\xi_{t_{\mathrm{max}}}^2$. The second moment of the distribution is the case $k = 2$, which reads

$$
\begin{aligned}
<t^2> &= -\exp(-t_{\mathrm{max}}^2/s^2 - t_{\mathrm{ub}}^2/s^2 - t_{\mathrm{lb}}^2/s^2)(2s^2 t_{\mathrm{max}}\exp(t_{\mathrm{ub}}^2/s^2 \\
&\quad +(2t_{\mathrm{max}}t_{\mathrm{lb}})/s^2) + 2s^2 t_{\mathrm{lb}}\exp(t_{\mathrm{ub}}^2/s^2 \\
&\quad +(2t_{\mathrm{max}}t_{\mathrm{lb}})/s^2) - 2s^2 t_{\mathrm{max}}\exp((2t_{\mathrm{max}}t_{\mathrm{ub}})/s^2 \\
&\quad +t_{\mathrm{lb}}^2/s^2) - 2s^2 t_{\mathrm{ub}}\exp((2t_{\mathrm{max}}t_{\mathrm{ub}})/s^2 + t_{\mathrm{lb}}^2/s^2) \\
&\quad -\sqrt{\pi}s^3\mathrm{erfc}((t_{\mathrm{ub}} - t_{\mathrm{max}})/s)\exp(t_{\mathrm{max}}^2/s^2 \\
&\quad +t_{\mathrm{ub}}^2/s^2 + t_{\mathrm{lb}}^2/s^2) \\
&\quad -2\sqrt{\pi}st_{\mathrm{max}}^2\mathrm{erfc}((t_{\mathrm{ub}} - t_{\mathrm{max}})/s)\exp(t_{\mathrm{max}}^2/s^2 \\
&\quad +t_{\mathrm{ub}}^2/s^2 + t_{\mathrm{lb}}^2/s^2) + \sqrt{\pi}s^3\exp(t_{\mathrm{max}}^2/s^2 + t_{\mathrm{ub}}^2/s^2 \\
&\quad +t_{\mathrm{lb}}^2/s^2)\mathrm{erfc}((t_{\mathrm{lb}} - t_{\mathrm{max}})/s) \\
&\quad +2\sqrt{\pi}st_{\mathrm{max}}^2\exp(t_{\mathrm{max}}^2/s^2 + t_{\mathrm{ub}}^2/s^2 \\
&\quad +t_{\mathrm{lb}}^2/s^2)\mathrm{erfc}((t_{\mathrm{lb}} - t_{\mathrm{max}})/s))/2.
\end{aligned}
\qquad (S32)
$$

The dispersion of $t$ is calculated as

$$\xi_t = (<t^2>/t_0^2 - 1)^{1/2}. \qquad (S33)$$

## S6 Average number of stacked platelets over a Gaussian distribution comprised between two bounds

The Gaussian distribution function of the number $N_c$ of stacked platelets is

$$p_{N_c}(N_c) = \frac{1}{Z_{N_c}}e^{-(N_c-N_{c,\mathrm{max}})^2/(2\sigma_{N_c}^2)} \tag{S34}$$

The normalization factor $Z_t$ is determined by the following equation

$$\begin{aligned}
Z_{N_c} &= \int_{N_{c,\mathrm{lb}}}^{N_{c,\mathrm{ub}}} e^{-(N_c-N_{c,\mathrm{max}})^2/(2\sigma_{N_c}^2)}dN_c \\
&= \sigma_{N_c}\sqrt{\frac{\pi}{2}}\left[\mathrm{erf}\left(\frac{N_{c,\mathrm{ub}}-N_{c,\mathrm{max}}}{\sqrt{2}\sigma_{N_c}}\right) - \mathrm{erf}\left(\frac{N_{c,\mathrm{lb}}-N_{c,\mathrm{max}}}{\sqrt{2}\sigma_{N_c}}\right)\right].
\end{aligned} \tag{S35}$$

where $N_{c,\mathrm{lb}} = \max\{N_{c,\mathrm{max}}-p_G\sigma_{N_c}, N_{c,\mathrm{min}}\}$ and $N_{c,\mathrm{ub}} = N_{c,\mathrm{max}}+p_G\sigma_{N_c}$ are the lower and the upper bounds of the integrals and $N_{c,\mathrm{min}}$ is the minimum allowed value of the lower integration bound, which was fixed to $N_{c,\mathrm{min}} = 1$. The average number of stacked platelets is

$$\begin{aligned}
N_{c,0} &= \int_{N_{c,\mathrm{lb}}}^{N_{c,\mathrm{ub}}} N_c\, p_{N_c}(N_c)\, dN_c = \frac{G_5}{Z_{N_c}} \\
G_5 &= \sqrt{2\pi}N_{c,\mathrm{max}}\sigma_{N_c} \\
&\quad +\sigma_{N_c}^2\left(e^{-(N_{c,\mathrm{lb}}-N_{c,\mathrm{max}})^2/(2\sigma_{N_c}^2)} - e^{-(N_{c,\mathrm{ub}}-N_{c,\mathrm{max}})^2/(2\sigma_{N_c}^2)}\right) \\
&\quad +N_{c,\mathrm{max}}\sigma_{N_c}\sqrt{\frac{\pi}{2}}\left[\mathrm{erfc}\left(\frac{N_{c,\mathrm{lb}}-N_{c,\mathrm{max}}}{\sqrt{2}\sigma_{N_c}}\right) - \mathrm{erfc}\left(\frac{N_{c,\mathrm{ub}}-N_{c,\mathrm{max}}}{\sqrt{2}\sigma_{N_c}}\right)\right]
\end{aligned} \tag{S36}$$

## S7 Distribution function of the center-to-border distance of a polydisperse barrel

For a barrel with minimum and maximum circular cross-section radius $\nu R_M$ and $R_M$, respectively, and with height $H$, the distance from the center and the border taken along a direction that forms an angle $\beta$ with the barrel axis is given by the function

$$f_c(\beta) = \begin{cases} \frac{H}{2\cos\beta} & 0 \le \beta \le \tan^{-1}\left(\frac{2\nu R_M}{H}\right) \\ \frac{HR_M\left[H\nu\tan\beta+(1-\nu)\sqrt{4(1-2\nu)R_M^2+H^2\tan^2\beta}\right]}{\cos\beta\left[4(1-\nu)^2R_M^2+H^2\tan^2\beta\right]} & 0 < \beta < \tan^{-1}\left(\frac{2\nu R_M}{H}\right) \\ R_M & \beta = \frac{\pi}{2} \end{cases} \tag{S37}$$

Hence, the average center-to-border distance is the zenith integral

$$R_{\rm c} \;\; = \;\; \int_0^{\pi/2} d\beta \, \sin\beta \, f_{\rm c}(\beta) \tag{S38}$$

For a polydisperse barrel over both $R_M$ and $H$, the probability density of the center-to-border distance, $p(R_{\rm c})$, is obtained by sampling $R_M$ and $H$ over the two corresponding distribution functions $p(R_M)$ and $p(H)$ determined by the analysis of SAXS data. A simple Monte Carlo method that samples 300000 values of $R_{\rm c}$ has been developed for this aim.

## S8 SAXS amplitude of $3$ specular layers of electron densities with smooth transitions

The excess ED profile, relative to the average ED of the entire barrel ($\rho_{\rm brl}$, see Eq. S122), of 3 specular layers with smooth transitions along the $z$ direction perpendicular to the layers is[2]

$$\delta\rho_f(z) \;\; = \;\; \sum_{j=1}^{3} (\rho_{f,j} - \rho_{f,j-1}) E(z, z_j, \sigma_{{\rm pl},j}) \tag{S39}$$

where $\rho_{f,0} = \rho_{\rm brl}$, the indexes $j = 1, 2, 3$ correspond to the outer, middle, and inner domains, the $z$ levels are $z_j = t + \tau_j$, with, by definition, $\tau_1 = t_1 + t_2$, $\tau_2 = t_2$ and $\tau_3 = 0$. The smoothness parameter on going from the $j$-layer to the $(j-1)$-layer is $\sigma_{{\rm pl},j}$. The function $E(z, z_0, \sigma)$ represents a combination of two symmetrical error functions[3],

$$E(z, z_0, \sigma) = \frac{1}{2}\left[\mathrm{erf}\left(\frac{z+z_0}{2^{1/2}\sigma}\right) - \mathrm{erf}\left(\frac{z-z_0}{2^{1/2}\sigma}\right)\right] \tag{S40}$$

A representative plot of $\delta\rho_f(z)$ is shown in Fig. S4. To note, the volume fraction distributions along $z$ of the three domains are,

$$\varphi_1(z) \;\; = \;\; E(z, z_1, \sigma_{{\rm pl},1}) - E(z, z_2, \sigma_{{\rm pl},2}) \tag{S41}$$

$$\varphi_2(z) \;\; = \;\; E(z, z_2, \sigma_{{\rm pl},2}) - E(z, z_3, \sigma_{{\rm pl},3}) \tag{S42}$$

$$\varphi_3(z) \;\; = \;\; E(z, z_3, \sigma_{{\rm pl},3}) \tag{S43}$$

Details on the calculation of the electron densities $\rho_{f,j}$ in Eq. S39 on the basis of the composition

of the platelet are shown in Sect. S11.3.2 (Eqs. S65, S115, S116, S117).

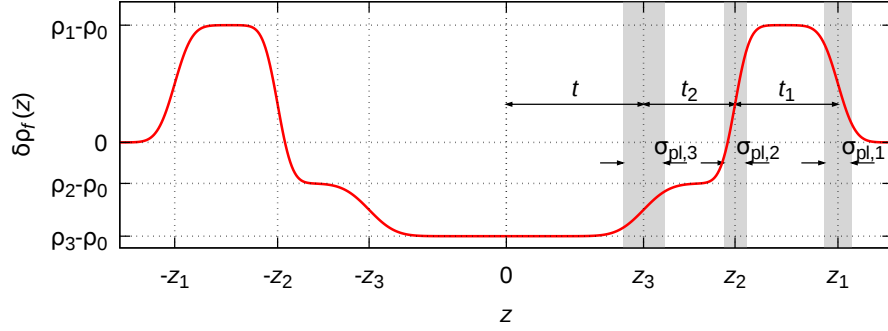The one-dimensional Fourier transform of Eq. S39 reads



Figure S4: Excess ED calculated with Eq. S39.

$$A_{\mathrm{fl},f}(q) = 2\sum_{j=1}^{3} z_j (\rho_{f,j} - \rho_{f,j-1}) \frac{\sin(qz_j)}{qz_j} e^{-q^2\sigma_{\mathrm{pl},j}^2/2} \tag{S44}$$

Eq. S44 can be re-written in the more useful complex space according to

$$A_{\mathrm{fl},f}(q) = -\frac{i}{q}\sum_{j=1}^{3} (\rho_{f,j} - \rho_{f,j-1}) e^{-q^2\sigma_{\mathrm{pl},j}^2/2} (e^{iqz_j} - e^{-iqz_j}) \tag{S45}$$

The squared amplitude is

$$\begin{aligned} A_{\mathrm{fl},f}^2(q) &= \frac{1}{q^2}\sum_{j_1=1}^{3}\sum_{j_2=1}^{3} (\rho_{f,j_1} - \rho_{f,j_1-1}) e^{-q^2\sigma_{j_1}^2/2} (\rho_{f,j_2} - \rho_{f,j_2-1}) e^{-q^2\sigma_{j_2}^2/2} \\ &\quad (e^{iq(2t+\tau_{j_1}+\tau_{j_2})} - e^{iq(\tau_{j_1}-\tau_{j_2})} - e^{-iq(\tau_{j_1}-\tau_{j_2})} + e^{-iq(2t+\tau_{j_1}+\tau_{j_2})}) \end{aligned} \tag{S46}$$

The averages $<(t+t_2)^{-1}A_{\mathrm{fl},f}^2(q)>_t$, which enter into Eq. 18, read

$$
\begin{aligned}
<(t+t_2)^{-1}A_{\mathrm{fl},f}^2(q)>_t \;=\; & \frac{1}{q^2}\sum_{j_1=1}^{3}(\rho_{f,j_1}-\rho_{f,j_1-1})^2 e^{-q^2\sigma_{j_1}^2} \\
& (e^{i2q\tau_{j_1}}<(t+t_2)^{-1}e^{2iqt}>_t -2<(t+t_2)^{-1}>_t \\
& +e^{-i2q\tau_{j_1}}<(t+t_2)^{-1}e^{-2iqt}>_t) \\
& +\frac{2}{q^2}\sum_{j_1=1}^{2}\sum_{j_2=j_1+1}^{3}(\rho_{f,j_1}-\rho_{f,j_1-1})(\rho_{f,j_2}-\rho_{f,j_2-1})e^{-q^2(\sigma_{j_1}^2+\sigma_{j_2}^2)/2} \\
& (e^{iq(\tau_{j_1}+\tau_{j_2})}<(t+t_2)^{-1}e^{2iqt}>_t -(e^{iq(\tau_{j_1}-\tau_{j_2})} \\
& +e^{-iq(\tau_{j_1}-\tau_{j_2})})<(t+t_2)^{-1}>_t \\
& +e^{-iq(\tau_{j_1}+\tau_{j_2})}<(t+t_2)^{-1}e^{-2iqt}>_t)
\end{aligned}
\tag{S47}
$$

We have calculated the term $<(t+t_2)^{-1}e^{iqkt}>_t$ by sampling the Gaussian distribution seen in Eq. S30 over $n_t$ points and by performing an analytical integration over the piecewise lines according to

$$
\begin{aligned}
<(t+t_2)^{-1}e^{iqkt}>_t =\; & \frac{1}{Z_t}\int_{t_{\mathrm{lb}}}^{t_{\mathrm{ub}}}(t+t_2)^{-1}e^{iqkt}e^{-(t-t_{\max})^2/(2\xi_{t_{\max}}^2 t_{\max}^2)}dt \\
\approx\; & \frac{1}{Z_t}\frac{1}{q^2k^2\Delta t}\sum_{j=1}^{n_t-1}((1-iqk\Delta t)e^{iqkt_{j+1}}-e^{iqkt_j})(t_{j+1}+t_2)^{-1}e^{-(t_{j+1}-t_{\max})^2/(2\xi_{t_{\max}}^2 t_{\max}^2)} \\
& +((1+iqk\Delta t)e^{iqkt_j}-e^{iqkt_{j+1}})(t_j+t_2)^{-1}e^{-(t_j-t_{\max})^2/(2\xi_{t_{\max}}^2 t_{\max}^2)}
\end{aligned}
\tag{S48}
$$

where the sampled points are $t_j = t_{\mathrm{lb}}+(j-1)\Delta t$, with $\Delta t=(t_{\mathrm{ub}}-t_{\mathrm{lb}})/(n_t-1)$.

## S9  Calculation of the radial averages of Eq. 18

The three radial averages shown in Eq. 18, which involve the following three functions,

$$
F_1(R) = t_1(t_1+2(R+t_2))(R+t_2)^{-2}, \tag{S49}
$$

$$
F_2(R) = t_2(t_2+2R)(R+t_2)^{-2}, \tag{S50}
$$

$$
F_3(R) = R^2(R+t_2)^{-2}, \tag{S51}
$$

are defined by the following integral

$$
\begin{aligned}
<F_k(R)>_R &= \int_{\nu R_{M,\text{lb}}}^{R_{M,\text{ub}}} F_k(R)\, p(R) dR \\
&= \frac{1}{Z_{R_M}} \int_{R_{M,\text{lb}}}^{R_{M,\text{ub}}} F_{k,a}(R_M)\, e^{-(R_M - R_{M,\text{max}})^2/(2\xi_{R_M}^2 R_{M,\text{max}}^2)} dR_M,
\end{aligned}
\tag{S52}
$$

where, considering the definition of $p(R, R_M, \nu R_M)$ (Eq. 11), we have introduced the following functions

$$
\begin{aligned}
F_{k,a}(R_M) &= \int_{\nu R_{M,\text{lb}}}^{R_{M,\text{ub}}} F_k(R) p(R, R_M, \nu R_M) dR \\
&= \int_{\nu R_M}^{R_M} F_k(R) p(R, R_M, \nu R_M) dR
\end{aligned}
\tag{S53}
$$

We have been able, by exploiting the computer algebra system Maxima[4], to analytically solve the integrals shown in Eq. S53. Results, for the case $R_M(2\nu - 1) + t_2 \geq 0$, are given by the following

relationships:

$$
\begin{aligned}
F_{1,a}(R_M) \;=\; & -(\sqrt{R_M + t_2}\sqrt{2R_M\nu - R_M + t_2}(2\pi \\
& t_2^3 t_1 + (\pi t_1^2 - 2\pi t_2 t_1)R_M^2 + ((-2\pi t_1 \\
& R_M^3) + (4\pi t_2 t_1 - 2\pi t_1^2)R_M^2 + 6\pi t_2^2 t_1 \\
& R_M)\nu + (4\pi t_1 R_M^3 + (4\pi t_2 t_1 + \pi t_1^2) \\
& R_M^2)\nu^2 + (((2t_1^2 + 8t_2 t_1)R_M^2 + 8t_1 R_M^3)\nu^2 + (12t_2^2 \\
& t_1 R_M + (8t_2 t_1 - 4t_1^2)R_M^2 - 4t_1 R_M^3)\nu + (2t_1^2 - 4 \\
& t_2 t_1)R_M^2 + 4t_2^3 t_1)\sin^{-1}((R_M\nu - R_M)/(t_2 + R_M \\
& \nu))) + ((4t_2 t_1^2 - 8\pi t_2^2 t_1)R_M^2 + (4t_1^2 - 16\pi t_2 \\
& t_1)R_M^3 - 8\pi t_1 R_M^4)\nu^2 + ((2t_2^2 t_1^2 - 8\pi t_2^3 \\
& t_1)R_M + ((-4t_2 t_1^2) - 8\pi t_2^2 t_1)R_M^2 + (8\pi t_2 \\
& t_1 - 6t_1^2)R_M^3 + 8\pi t_1 R_M^4)\nu - 2\pi t_1 R_M^4 + 2 \\
& t_1^2 R_M^3 + 4\pi t_2^2 t_1 R_M^2 - 2t_2^2 t_1^2 R_M - 2\pi \\
& t_2^4 t_1)/((-2t_2^4 R_M) + 4t_2^2 R_M^3 - 2R_M^5 + (10R_M^5 + 8t_2 R_M^4 - 12 \\
& t_2^2 R_M^3 - 8t_2^3 R_M^2 + 2t_2^4 R_M)\nu + ((-16R_M^5) - 24t_2 R_M^4 + 8 \\
& t_2^3 R_M^2)\nu^2 + (8R_M^5 + 16t_2 R_M^4 + 8t_2^2 R_M^3)\nu^3)
\end{aligned}
\tag{S54}
$$

$$
\begin{aligned}
F_{2,a}(R_M) \;=\; & -(\sqrt{R_M + t_2}\sqrt{2R_M\nu - R_M + t_2}(2\pi \\
& t_2^4 - 3\pi t_2^2 R_M^2 + ((-2\pi t_2 R_M^3) + 6\pi t_2^2 R_M^2 + 6 \\
& \pi t_2^3 R_M)\nu + (4\pi t_2 R_M^3 + 3\pi t_2^2 R_M^2) \\
& \nu^2 + ((6t_2^2 R_M^2 + 8t_2 R_M^3)\nu^2 + (12t_2^3 R_M + 12t_2^2 R_M^2 - 4 \\
& t_2 R_M^3)\nu - 6t_2^2 R_M^2 + 4t_2^4)\sin^{-1}((R_M\nu - R_M)/(t_2 + \\
& R_M\nu))) + (((-8\pi) - 4)t_2^3 R_M^2 + ((-16\pi) - 4)t_2^2 R_M^3 - 8\pi t_2 \\
& R_M^4)\nu^2 + (((-8\pi) - 2)t_2^4 R_M + (4 - 8\pi)t_2^3 R_M^2 + (8\pi + 6)t_2^2 \\
& R_M^3 + 8\pi t_2 R_M^4)\nu - 2\pi t_2 R_M^4 - 2t_2^2 R_M^3 + 4 \\
& \pi t_2^3 R_M^2 + 2t_2^4 R_M - 2\pi t_2^5)/((-2t_2^4 R_M) + 4t_2^2 \\
& R_M^3 - 2R_M^5 + (10R_M^5 + 8t_2 R_M^4 - 12t_2^2 R_M^3 - 8t_2^3 R_M^2 + 2t_2^4 \\
& R_M)\nu + ((-16R_M^5) - 24t_2 R_M^4 + 8t_2^3 R_M^2)\nu^2 + (8R_M^5 + 16t_2 \\
& R_M^4 + 8t_2^2 R_M^3)\nu^3)
\end{aligned}
\tag{S55}
$$

$$
\begin{aligned}
F_{3,a}(R_M) \;=\; & (\sqrt{R_M + t_2}\sqrt{2R_M\nu - R_M + t_2}(2\pi \\
& t_2^4 - 3\pi t_2^2 R_M^2 + ((-2\pi t_2 R_M^3) + 6\pi t_2^2 R_M^2 + 6 \\
& \pi t_2^3 R_M)\nu + (4\pi t_2 R_M^3 + 3\pi t_2^2 R_M^2) \\
& \nu^2 + ((6t_2^2 R_M^2 + 8t_2 R_M^3)\nu^2 + (12t_2^3 R_M + 12t_2^2 R_M^2 - 4 \\
& t_2 R_M^3)\nu - 6t_2^2 R_M^2 + 4t_2^4)\sin^{-1}((R_M\nu - R_M)/(t_2 + \\
& R_M\nu))) + ((-8t_2^2 R_M^3) - 16t_2 R_M^4 - 8R_M^5)\nu^3 + (((-8\pi) - 12)t_2^3 \\
& R_M^2 + ((-16\pi) - 4)t_2^2 R_M^3 + (24 - 8\pi)t_2 R_M^4 + 16R_M^5)\nu^2 + (((-8\pi) - 4) \\
& t_2^4 R_M + (12 - 8\pi)t_2^3 R_M^2 + (8\pi + 18)t_2^2 R_M^3 + (8\pi - 8)t_2 \\
& R_M^4 - 10R_M^5)\nu + 2R_M^5 - 2\pi t_2 R_M^4 - 6t_2^2 R_M^3 + 4\pi \\
& t_2^3 R_M^2 + 4t_2^4 R_M - 2\pi t_2^5)/((-2t_2^4 R_M) + 4t_2^2 R_M^3 - 2 \\
& R_M^5 + (10R_M^5 + 8t_2 R_M^4 - 12t_2^2 R_M^3 - 8t_2^3 R_M^2 + 2t_2^4 R_M) \\
& \nu + ((-16R_M^5) - 24t_2 R_M^4 + 8t_2^3 R_M^2)\nu^2 + (8R_M^5 + 16t_2 R_M^4 + 8 \\
& t_2^2 R_M^3)\nu^3)
\end{aligned}
\tag{S56}
$$

On the other hand, for $R_M(2\nu - 1) + t_2 < 0$, the functions $F_{k,a}(R_M)$ are:

$$
\begin{aligned}
F_{1,a}(R_M) = & -(\sqrt{R_M + t_2}\sqrt{(-2R_M\nu) + R_M - t_2}((-2i \\
& \pi t_2^3 t_1) + (2i\pi t_2 t_1 - i\pi t_1^2) \\
& R_M^2 + (2i\pi t_1 R_M^3 + (2i\pi t_1^2 - 4i\pi \\
& t_2 t_1)R_M^2 - 6i\pi t_2^2 t_1 R_M)\nu + (((-4i \\
& \pi t_2 t_1) - i\pi t_1^2)R_M^2 - 4i\pi t_1 \\
& R_M^3)\nu^2 + ((((-t_1^2) - 4t_2 t_1)R_M^2 - 4t_1 R_M^3)\nu^2 + ((-6t_2^2 \\
& t_1 R_M) + (2t_1^2 - 4t_2 t_1)R_M^2 + 2t_1 R_M^3)\nu + (2t_2 \\
& t_1 - t_1^2)R_M^2 - 2t_2^3 t_1)\log(R_M\nu + t_2) + (((t_1^2 + 4 \\
& t_2 t_1)R_M^2 + 4t_1 R_M^3)\nu^2 + (6t_2^2 t_1 R_M + (4t_2 \\
& t_1 - 2t_1^2)R_M^2 - 2t_1 R_M^3)\nu + (t_1^2 - 2t_2 t_1)R_M^2 + 2 \\
& t_2^3 t_1)\log(\sqrt{R_M + t_2}\sqrt{(-2R_M\nu) + R_M - t_2} + \\
& R_M\nu - R_M))) + ((2t_2 t_1^2 - 4\pi t_2^2 t_1)R_M^2 + (2 \\
& t_1^2 - 8\pi t_2 t_1)R_M^3 - 4\pi t_1 R_M^4)\nu^2 + ((t_2^2 \\
& t_1^2 - 4\pi t_2^3 t_1)R_M + ((-2t_2 t_1^2) - 4\pi t_2^2 t_1) \\
& R_M^2 + (4\pi t_2 t_1 - 3t_1^2)R_M^3 + 4\pi t_1 R_M^4)\nu - \\
& \pi t_1 R_M^4 + t_1^2 R_M^3 + 2\pi t_2^2 t_1 R_M^2 - t_2^2 \\
& t_1^2 R_M - \pi t_2^4 t_1)/((-t_2^4 R_M) + 2t_2^2 R_M^3 - R_M^5 + (5 \\
& R_M^5 + 4t_2 R_M^4 - 6t_2^2 R_M^3 - 4t_2^3 R_M^2 + t_2^4 R_M)\nu + ((-8 \\
& R_M^5) - 12t_2 R_M^4 + 4t_2^3 R_M^2)\nu^2 + (4R_M^5 + 8t_2 R_M^4 + 4t_2^2 R_M^3)\nu^3) \qquad \text{(S57)}
\end{aligned}
$$

$$
\begin{aligned}
F_{2,a}(R_M) \;=\; & -(\sqrt{R_M + t_2}\sqrt{(-2R_M\nu) + R_M - t_2}((-2i \\
& \pi t_2^4) + 3i\pi t_2^2 R_M^2 + (2i\pi t_2 R_M^3 - 6 \\
& i\pi t_2^2 R_M^2 - 6i\pi t_2^3 R_M)\nu + ((-4i \\
& \pi t_2 R_M^3) - 3i\pi t_2^2 R_M^2)\nu^2 + (((-3t_2^2 R_M^2) - 4 \\
& t_2 R_M^3)\nu^2 + ((-6t_2^3 R_M) - 6t_2^2 R_M^2 + 2t_2 R_M^3)\nu + 3 \\
& t_2^2 R_M^2 - 2t_2^4)\log(R_M\nu + t_2) + ((3t_2^2 R_M^2 + 4t_2 \\
& R_M^3)\nu^2 + (6t_2^3 R_M + 6t_2^2 R_M^2 - 2t_2 R_M^3)\nu - 3t_2^2 \\
& R_M^2 + 2t_2^4)\log((\sqrt{R_M + t_2}\sqrt{(-2R_M\nu) + R_M - t_2} + \\
& R_M\nu - R_M))) + (((-4\pi) - 2)t_2^3 R_M^2 + ((-8\pi) - 2)t_2^2 R_M^3 - 4 \\
& \pi t_2 R_M^4)\nu^2 + (((-4\pi) - 1)t_2^4 R_M + (2 - 4\pi)t_2^3 R_M^2 + (4 \\
& \pi + 3)t_2^2 R_M^3 + 4\pi t_2 R_M^4)\nu - \pi t_2 R_M^4 - \\
& t_2^2 R_M^3 + 2\pi t_2^3 R_M^2 + t_2^4 R_M - \pi t_2^5)/((-t_2^4 \\
& R_M) + 2t_2^2 R_M^3 - R_M^5 + (5R_M^5 + 4t_2 R_M^4 - 6t_2^2 R_M^3 - 4t_2^3 \\
& R_M^2 + t_2^4 R_M)\nu + ((-8R_M^5) - 12t_2 R_M^4 + 4t_2^3 R_M^2)\nu^2 + (4 \\
& R_M^5 + 8t_2 R_M^4 + 4t_2^2 R_M^3)\nu^3)
\end{aligned}
\tag{S58}
$$

$$
\begin{aligned}
F_{3,a}(R_M) \;=\; & (\sqrt{R_M + t_2}\sqrt{(-2R_M\nu) + R_M - t_2}((-2i \\
& \pi t_2^4) + 3i\pi t_2^2 R_M^2 + (2i\pi t_2 R_M^3 - 6 \\
& i\pi t_2^2 R_M^2 - 6i\pi t_2^3 R_M)\nu + ((-4i \\
& \pi t_2 R_M^3) - 3i\pi t_2^2 R_M^2)\nu^2 + (((-3t_2^2 R_M^2) - 4 \\
& t_2 R_M^3)\nu^2 + ((-6t_2^3 R_M) - 6t_2^2 R_M^2 + 2t_2 R_M^3)\nu + 3 \\
& t_2^2 R_M^2 - 2t_2^4)\log(R_M\nu + t_2) + ((3t_2^2 R_M^2 + 4t_2 \\
& R_M^3)\nu^2 + (6t_2^3 R_M + 6t_2^2 R_M^2 - 2t_2 R_M^3)\nu - 3t_2^2 \\
& R_M^2 + 2t_2^4)\log((\sqrt{R_M + t_2}\sqrt{(-2R_M\nu) + R_M - t_2} + \\
& R_M\nu - R_M))) + ((-4t_2^2 R_M^3) - 8t_2 R_M^4 - 4R_M^5)\nu^3 + (((-4 \\
& \pi) - 6)t_2^3 R_M^2 + ((-8\pi) - 2)t_2^2 R_M^3 + (12 - 4\pi)t_2 R_M^4 + 8R_M^5) \\
& \nu^2 + (((-4\pi) - 2)t_2^4 R_M + (6 - 4\pi)t_2^3 R_M^2 + (4\pi + 9)t_2^2 R_M^3 + (4 \\
& \pi - 4)t_2 R_M^4 - 5R_M^5)\nu + R_M^5 - \pi t_2 R_M^4 - 3t_2^2 \\
& R_M^3 + 2\pi t_2^3 R_M^2 + 2t_2^4 R_M - \pi t_2^5)/((-t_2^4 R_M) + 2 \\
& t_2^2 R_M^3 - R_M^5 + (5R_M^5 + 4t_2 R_M^4 - 6t_2^2 R_M^3 - 4t_2^3 R_M^2 + \\
& t_2^4 R_M)\nu + ((-8R_M^5) - 12t_2 R_M^4 + 4t_2^3 R_M^2)\nu^2 + (4R_M^5 + 8 \\
& t_2 R_M^4 + 4t_2^2 R_M^3)\nu^3)
\end{aligned}
\tag{S59}
$$

Notice that Eqs. S57-S59 have been solved in the complex space so that, for example, the logarithmic functions are applied to negative numbers. However, we have checked that the imaginary part of all the expressions is zero. Finally, the integral averages $< F_k(R) >_R$ over a Gaussian (shown in Eq. S52) are numerically calculated with the Simpson's rule by using 10 points.

## S10   SAXS amplitude of 3-electron density levels of CP bilayers with smooth transitions

The excess ED profile of 3 specular layers of EDs with smooth transitions along the $z$ direction perpendicular to the layers, representing the $k$-th nano-crystal region of CP (see Fig. 3, panels C

and D), is[2]

$$\delta\rho_k(z) \;=\; \sum_{i=1}^{3}(\rho_{k,i}-\rho_{k,i-1})E(z,z_k,\sigma_{k,i}) \tag{S60}$$

where $\rho_{\mathrm{CP},0}$ is the average CP ED, according to

$$\rho_{k,0} = \frac{\sum_{i=1}^{3}\nu_{\mathrm{CP},i}\rho_{\mathrm{CP},i}}{\sum_{i=1}^{3}\nu_{\mathrm{CP},i}} \tag{S61}$$

In this equation, $\nu_{\mathrm{CP},i}$ and $\rho_{\mathrm{CP},i}$ are the molecular volume and the ED of the carboxyl group ($i=1$), the middle ($i=2$) and the terminal ($i=3$) chains of the CP molecules, respectively. The $z$ levels are $z_i = \sum_{i'=i}^{3}\delta_{k,i'}$ and $\sigma_{k,i}$ is the smoothness parameter on going from the $i$-layer to the ($i-1$)-layer. A representative plot of $\delta\rho_k(z)$ is shown in Fig. S5. The one-dimensional Fourier transform of Eq. S60 reads

$$A_{\mathrm{ld},k}(q) = 2\sum_{i=1}^{3} z_i(\rho_{k,i}-\rho_{k,i-1})\frac{\sin(qz_i)}{qz_i}e^{-q^2\sigma_{k,i}^2/2} \tag{S62}$$
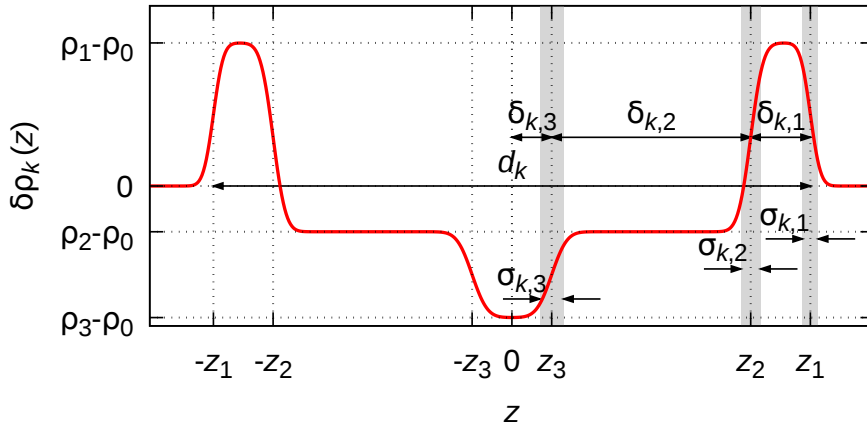


Figure S5: Excess ED calculated with Eq. S60.

Electron densities $\rho_{k,i}$ and thicknesses $\delta_{k,i}$ are calculated according to the physical-chemical characteristics of the groups forming the CP molecule, shown in Table 2. Explicit equations are reported in the Sect. S11.3.1, Eqs. S85, S86, S90, S91, S92, S93, S94, S96, S97, S98, S99, S100 and S101.

# S11 Volumetric constraints and calculation of electron densities

## S11.1 Water and thermal expansivities

The relative mass density of bulk water is calculated as a function of $T$ with the following expression

$$d_{\text{wat}} = e^{-\alpha_{\text{wat}}(T-T_\circ)-\beta_{\text{wat}}(T-T_\circ)^2/2}, \tag{S63}$$

where the thermal expansivity of water at $T_\circ$ and its first derivative are $\alpha_{\text{wat}} = 2.5 \cdot 10^{-4}\ \text{K}^{-1}$ and $\beta_{\text{wat}} = 9.8 \cdot 10^{-6}\ \text{K}^{-2}$, respectively[5]. Conversely, the temperature dependency of the relative mass density of both CP and P80 molecules is expressed as a function of the thermal expansivity $\alpha_{\text{lip}}$ of lipids, according to

$$d_{\text{lip}} = e^{-\alpha_{\text{lip}}(T-T_\circ)}, \tag{S64}$$

$\alpha_{\text{lip}}$ being considered an adjustable parameter.

The bulk water electron density is

$$\rho_0 = e_{\text{H}_2\text{O}}/(\nu_{\text{wat}}^\circ/d_{\text{wat}}) \tag{S65}$$

## S11.2 End-capped cylindrical micelles

The molecular volume of the hydrophobic region of P80 is

$$\nu_{\text{P80,hyd}} = (14\nu_{\text{CH}_2} + 2\nu_{\text{CH}} + \nu_{\text{CH}_3})/d_{\text{lip}}. \tag{S66}$$

The molecular volume of the dry polar region of P80 is written as

$$\nu_{\text{P80,pol,dry}} = ((2\nu_{\text{CH}_2} + \nu_{-\text{O}-})20 + \nu_{>\text{C}=} + 2\nu_{-\text{O}-} + \nu_{\text{O}=} + 2\nu_{\text{CH}_2} + 4\nu_{\text{CH}} + 3\nu_{\text{OH}})/d_{\text{lip}}. \tag{S67}$$

The number of water molecules *per* molecule of P80 in $(k = 1)$ domain (see Eq. S12, here

referred to as 1-domain) of the end-cap region of the micelle is derived by the following equation

$$
\begin{aligned}
r_{\text{wat,cap}} \;=\; & (2\delta_{\text{cap}}^{3}\nu_{\text{P80,hyd}} + 6R_{2,\text{cap}}\delta_{\text{cap}}^{2}\nu_{\text{P80,hyd}} \\
& +3h\delta_{\text{cap}}^{2}\nu_{\text{P80,hyd}} + 6R_{2,\text{cap}}^{2}\delta_{\text{cap}}\nu_{\text{P80,hyd}} \\
& +6hR_{2,\text{cap}}\delta_{\text{cap}}\nu_{\text{P80,hyd}} - 2R_{2,\text{cap}}^{3}\nu_{\text{P80,pol,dry}} \\
& -3hR_{2,\text{cap}}^{2}\nu_{\text{P80,pol,dry}} + h^{3}\nu_{\text{P80,pol,dry}})/ \\
& ((h + R_{2,\text{cap}})^{2}(2R_{2,\text{cap}} - h)\nu_{\text{wat}}^{\circ}/d_{\text{wat}}/\hat{d}_{\text{wat,cap}}) \qquad (\text{S68})
\end{aligned}
$$

The number of water molecules *per* molecule of P80 in 1-domain of the cylinder region of the micelle is derived by the following equation

$$
r_{\text{wat,cyl}} = \frac{\delta_{\text{cap}}^{2}\nu_{\text{P80,hyd}} + 2R_{2,\text{cap}}\delta_{\text{cap}}\nu_{\text{P80,hyd}} - R_{2,\text{cap}}^{2}\nu_{\text{P80,pol,dry}} + h^{2}\nu_{\text{P80,pol,dry}}}{(R_{2,\text{cap}} - h)(h + R_{2,\text{cap}})\nu_{\text{wat}}^{\circ}/d_{\text{wat}}/\hat{d}_{\text{wat,cyl}}} \qquad (\text{S69})
$$

Accordingly, the electron densities of the 1-domain of the end-cap and of the cylinder regions of the micelle are

$$
\begin{aligned}
\rho_{1,\text{cap}} \;=\; & ((2e_{\text{CH}_2} + e_{-\text{O}-})20 + e_{>\text{C}=} \\
& +2e_{-\text{O}-} + e_{\text{O}=} + 2e_{\text{CH}_2} + 4e_{\text{CH}} + 3e_{\text{OH}} + r_{\text{wat,cap}}e_{\text{H}_2\text{O}}) \\
& /(\nu_{\text{P80,pol,dry}} + r_{\text{wat,cap}}\nu_{\text{wat}}^{\circ}/d_{\text{wat}}/\hat{d}_{\text{wat,cap}}) \qquad (\text{S70}) \\
\rho_{1,\text{cyl}} \;=\; & ((2e_{\text{CH}_2} + e_{-\text{O}-})20 + e_{>\text{C}=} \\
& +2e_{-\text{O}-} + e_{\text{O}=} + 2e_{\text{CH}_2} + 4e_{\text{CH}} + 3e_{\text{OH}} + r_{\text{wat,cyl}}e_{\text{H}_2\text{O}}) \\
& /(\nu_{\text{P80,pol,dry}} + r_{\text{wat,cyl}}\nu_{\text{wat}}^{\circ}/d_{\text{wat}}/\hat{d}_{\text{wat,cyl}}) \qquad (\text{S71})
\end{aligned}
$$

In Eqs. S68-S71, $\hat{d}_{\text{wat,cap}}$ and $\hat{d}_{\text{wat,cyl}}$ represent the relative mass density of water molecules embedded in the 1-domain of the end cap and the cylinder regions, respectively.

The electron density of the hydrophobic domain of the P80 molecule is

$$
\rho_{\text{P80,2}} = (14e_{\text{CH}_2} + 2e_{\text{CH}} + e_{\text{CH}_3})/\nu_{\text{P80,hyd}} \qquad (\text{S72})
$$

This ED corresponds to the ED of the 2-domain of both end-cap and cylinder regions of the micelle, $\rho_{2,\text{cap}}$ and $\rho_{2,\text{cyl}}$, respectively (see Eq. S12). The hydration of the 1-domain is calculated by the

ratio between the volume occupied by water and the total volume of the 1-domain, in both regions

$$\chi_{\text{cap}} = \frac{r_{\text{wat,cap}}\nu^{\circ}_{\text{wat}}/d_{\text{wat}}/\hat{d}_{\text{wat,cap}}}{\nu_{\text{P80,pol,dry}} + r_{\text{wat,cap}}\nu^{\circ}_{\text{wat}}/d_{\text{wat}}/\hat{d}_{\text{wat,cap}}} \tag{S73}$$

$$\chi_{\text{cyl}} = \frac{r_{\text{wat,cyl}}\nu^{\circ}_{\text{wat}}/d_{\text{wat}}/\hat{d}_{\text{wat,cyl}}}{\nu_{\text{P80,pol,dry}} + r_{\text{wat,cyl}}\nu^{\circ}_{\text{wat}}/d_{\text{wat}}/\hat{d}_{\text{wat,cyl}}} \tag{S74}$$

The area that each P80 molecule faces towards the water in the end-cap and the cylinder region can be calculated by the following expressions

$$a_{\text{P80,ec,cap,1}} = 3\frac{\nu_{\text{P80,hyd}}}{R_{2,\text{cap}}}\left(1 + \frac{\delta_{\text{cap}}}{R_{2,\text{cap}}}\right)^2 \frac{1 + \frac{h}{R_{2,\text{cap}}}}{1 + \frac{3}{2}\frac{h}{R_{2,\text{cap}}} - \frac{1}{2}\left(\frac{h}{R_{2,\text{cap}}}\right)^3} \tag{S75}$$

$$a_{\text{P80,ec,cyl,1}} = 2\frac{\nu_{\text{P80,hyd}}}{R_{2,\text{cyl}}}\left(1 + \frac{\delta_{\text{cyl}}}{R_{2,\text{cyl}}}\right) \tag{S76}$$

We can also calculate the corresponding areas at the interface between 1-domain and 2-domain in both regions. They are

$$a_{\text{P80,ec,cap,1,2}} = 3\frac{\nu_{\text{P80,hyd}}}{R_{2,\text{cap}}}\frac{1 + \frac{h}{R_{2,\text{cap}}}}{1 + \frac{3}{2}\frac{h}{R_{2,\text{cap}}} - \frac{1}{2}\left(\frac{h}{R_{2,\text{cap}}}\right)^3} \tag{S77}$$

$$a_{\text{P80,ec,cyl,1,2}} = 2\frac{\nu_{\text{P80,hyd}}}{R_{2,\text{cyl}}} \tag{S78}$$

### S11.3   Platelets

The molecular volume of CP, seen as a function of $T$, in the amorphous region (disordered chains, $\alpha$) is

$$\nu_{\text{CP},\alpha} = (29\nu_{\text{CH}_2} + 2\nu_{\text{CH}_3} + \nu_{>\text{C}=} + \nu_{-\text{O}-} + \nu_{\text{O}=})/d_{\text{lip}}. \tag{S79}$$

In the lamellar phases (ordered chains, $\beta$), the volume becomes

$$\nu_{\text{CP},\beta} = (29\nu_{\text{CH}_2}\beta_{\text{CH}_2} + 2\nu_{\text{CH}_3}\beta_{\text{CH}_3} + \nu_{>\text{C}=} + \nu_{-\text{O}-} + \nu_{\text{O}=})/d_{\text{lip}}, \tag{S80}$$

where $\beta_{\text{CH}_2}$ and $\beta_{\text{CH}_3}$ are, respectively, the reduction factors of volumes of the groups $CH_2$ and $CH_3$ in the ordered chains relative to the values they have in disordered chains.

### S11.3.1 Lamellar domains

The number of $CH_2$ groups of CP that are considered to be part of the $i = 1$ domain (see Eq. S60, shortly referred to as 1-domain) of each of the two lamellar phases are $N_{CH_2,CP,pol,1}$ and $N_{CH_2,CP,pol,2}$, respectively.

The fractions of $CH_2$ and $CH_3$ that occupy the $i = 2$ domain (see Eq. S60, shortly referred to as 2-domain) of the first lamellar phase are $x_{CP,CH_2,1}$ and $x_{CP,CH_3,1}$, respectively, where the fractions of $CH_2$ and $CH_3$ that occupies the 2-domain of the second lamellar phase are $x_{CP,CH_2,2}$ and $x_{CP,CH_3,2}$, respectively.

The number of correlated bilayers of the first and the second lamellar phase are $N_{CP,1}$ and $N_{CP,2}$, respectively, and the corresponding distortion factors are $g_{CP,1}$ and $g_{CP,2}$, respectively.

The areas associated with each CP molecule in the two lamellar phases are $a_{CP,1}$ and $a_{CP,2}$, respectively. These values allow us to calculate the repetition distance of two lamellar phases according to

$$d_1 = \nu_{CP,\beta}/a_{CP,1} \tag{S81}$$

$$d_2 = \nu_{CP,\beta}/a_{CP,2}. \tag{S82}$$

The volumes of the 1-domain of the CP molecule in the first and the second lamellar phase are,

$$\nu_{CP,1,1} = (1/d_{lip})(\nu_{>C=} + \nu_{-O-} + \nu_{O=} + N_{CH_2,CP,pol,1}\nu_{CH_2}\beta_{CH_2}) \tag{S83}$$

$$\nu_{CP,2,1} = (1/d_{lip})(\nu_{>C=} + \nu_{-O-} + \nu_{O=} + N_{CH_2,CP,pol,2}\nu_{CH_2}\beta_{CH_2}) \tag{S84}$$

and the two corresponding thicknesses are

$$\delta_{1,1} = \nu_{CP,1,1}/a_{CP,1} \tag{S85}$$

$$\delta_{2,1} = \nu_{CP,2,1}/a_{CP,2} \tag{S86}$$

The total volume of the $CH_2$ groups in both the 2-domain and the 3-domain of the CP in the first and in the second lamellar phases are

$$\nu_{CP,1,CH_2,2,3} = (29 - N_{CH_2,CP,pol,1})\nu_{CH_2}\beta_{CH_2}/d_{lip} \tag{S87}$$

$$\nu_{CP,2,CH_2,2,3} = (29 - N_{CH_2,CP,pol,2})\nu_{CH_2}\beta_{CH_2}/d_{lip} \tag{S88}$$

The total volume occupied by the $CH_3$ groups in the CP molecule is

$$\nu_{CP,CH_3} = 2\nu_{CH_3}\beta_{CH_3}/d_{lip} \tag{S89}$$

The thicknesses of the 2-domain the CP molecule in the first and in the second lamellar phase are

$$\delta_{1,2} = (\nu_{CP,1,CH_2,2,3}x_{CP,CH_2,1} + \nu_{CP,CH_3}x_{CP,CH_3,1})/a_{CP,1} \tag{S90}$$

$$\delta_{2,2} = (\nu_{CP,2,CH_2,2,3}x_{CP,CH_2,2} + \nu_{CP,CH_3}x_{CP,CH_3,2})/a_{CP,2} \tag{S91}$$

The thicknesses of the 3-domain the CP molecule in the first and in the second lamellar phase are

$$\delta_{1,3} = (\nu_{CP,1,CH_2,2,3}(1 - x_{CP,CH_2,1}) + \nu_{CP,CH_3}(1 - x_{CP,CH_3,1}))/a_{CP,1} \tag{S92}$$

$$\delta_{2,3} = (\nu_{CP,2,CH_2,2,3}(1 - x_{CP,CH_2,2}) + \nu_{CP,CH_3}(1 - x_{CP,CH_3,2}))/a_{CP,2} \tag{S93}$$

The average electron density of the CP molecule is

$$\rho_{CP,0} = \frac{e_C + 2e_O + 29e_{CH_2} + 2e_{CH_3}}{\bar{\nu}_{CP,3}}, \tag{S94}$$

where we have introduced the mean molecular volume of CP for ordered and disordered regions of the inner part of the platelet,

$$\bar{\nu}_{CP,3} = y_3\nu_{CP,\alpha} + (1 - y_3)\nu_{CP,\beta} \tag{S95}$$

The electron densities of the 1-domain of the first and the second lamellar phase are

$$\rho_{CP,1,1} = (e_C + 2e_O + e_{CH_2}N_{CH_2,CP,pol,1})/\nu_{CP,1,1} \tag{S96}$$

$$\rho_{CP,2,1} = (e_C + 2e_O + e_{CH_2}N_{CH_2,CP,pol,2})/\nu_{CP,2,1} \tag{S97}$$

The electron densities of the 2-domain of the first and the second lamellar phase are

$$\rho_{\text{CP},1,2} = \frac{x_{\text{CP,CH}_2,1}(29 - N_{\text{CH}_2,\text{CP,pol},1})e_{\text{CH}_2} + x_{\text{CP,CH}_3,1}2e_{\text{CH}_3}}{\nu_{\text{CP},1,\text{CH}_2,2,3}x_{\text{CP,CH}_2,1} + \nu_{\text{CP,CH}_3}x_{\text{CP,CH}_3,1}} \tag{S98}$$

$$\rho_{\text{CP},2,2} = \frac{x_{\text{CP,CH}_2,2}(29 - N_{\text{CH}_2,\text{CP,pol},2})e_{\text{CH}_2} + x_{\text{CP,CH}_3,2}2e_{\text{CH}_3}}{\nu_{\text{CP},2,\text{CH}_2,2,3}x_{\text{CP,CH}_2,2} + \nu_{\text{CP,CH}_3}x_{\text{CP,CH}_3,2}} \tag{S99}$$

The electron densities of the 3-domain of the first and the second lamellar phase are

$$\rho_{\text{CP},1,3} = \frac{(1 - x_{\text{CP,CH}_2,1})(29 - N_{\text{CH}_2,\text{CP,pol},1})e_{\text{CH}_2} + (1 - x_{\text{CP,CH}_3,1})2e_{\text{CH}_3}}{\nu_{\text{CP},1,\text{CH}_2,2,3}(1 - x_{\text{CP,CH}_2,1}) + \nu_{\text{CP,CH}_3}(1 - x_{\text{CP,CH}_3,1})} \tag{S100}$$

$$\rho_{\text{CP},2,3} = \frac{(1 - x_{\text{CP,CH}_2,2})(29 - N_{\text{CH}_2,\text{CP,pol},2})e_{\text{CH}_2} + (1 - x_{\text{CP,CH}_3,2})2e_{\text{CH}_3}}{\nu_{\text{CP},2,\text{CH}_2,2,3}(1 - x_{\text{CP,CH}_2,2}) + \nu_{\text{CP,CH}_3}(1 - x_{\text{CP,CH}_3,2})} \tag{S101}$$

### S11.3.2 Entire platelet

The nominal w/v concentration (in g/L) of nanoparticles, corresponding to both CP and P80 molecules in the sample, is indicated as $c_{\text{LNP}}$ and the nominal molar ratio between CP and P80 molecules as $r_{\text{CP,P80}}$. To each of these two parameters, we associate two correction factors, $k_{c_{\text{LNP}}}$ and $k_{r_{\text{CP,P80}}}$. Hence, the w/v concentration of CP in the sample is

$$c_{\text{CP}} = \frac{k_{c_{\text{LNP}}}c_{\text{LNP}}M_{\text{CP}}}{M_{\text{CP}} + M_{\text{P80}}/(k_{r_{\text{CP,P80}}}r_{\text{CP,P80}})}. \tag{S102}$$

The mass balance of CP and P80 is combined with the structural parameters of the platelet as follows. By referring to Fig. 3, the volumes of the platelet's core and the second (or intermediate) platelet's shell (labeled with $j = 2,3$ and $f = 2,3$) are related to the number of CP and P80 molecules in the platelet ($N_{\text{CP,pl}}$ and $N_{\text{P80,pl}}$, respectively) using

$$\sum_{f=2}^{3}\sum_{j=2}^{3}V_{f,j} = 2\pi(t + t_2)(R + t_2)^2$$

$$= N_{\text{CP,pl}}\bar{\nu}_{\text{CP}} + N_{\text{P80,pl}}\nu_{\text{P80,hyd}} \tag{S103}$$

where $\bar{\nu}_{\text{CP}}$ is the average molecular volume of CP in the platelet's core and the second platelet's shell. The number of P80 in the platelet can be expressed as a function of the fraction of P80 molecules embedded into the platelet, $y_{\text{P80}}$, and the nominal molar ratio between CP and P80

molecules, $r_{CP,P80}$ (a parameter known by the composition of the sample),

$$N_{P80,pl} = y_{P80} \frac{N_{CP,pl}}{r_{CP,P80} k_{r_{CP,P80}}}. \tag{S104}$$

Combining Eqs. S103-S104, we find $N_{CP,pl}$

$$N_{CP,pl} = \frac{2\pi(t + t_2)(R + t_2)^2}{\bar{\nu}_{CP} + \frac{\nu_{P80,hyd} y_{P80}}{r_{CP,P80} k_{r_{CP,P80}}}} \tag{S105}$$

The average value of $N_{CP,pl}$ over both the radial distribution $p(R)$ (Eq. 13) and the distribution of the half-thickness $p_t(t)$ (Eq. S28) is

$$<N_{CP,pl}> = \frac{2\pi(t_0 + t_2)(R_0^2(1 + \xi_R^2) + 2t_2 R_0 + t_2^2)}{\bar{\nu}_{CP} + \frac{\nu_{P80,hyd} y_{P80}}{r_{CP,P80} k_{r_{CP,P80}}}} \tag{S106}$$

Moreover, by considering only the volume of the second (intermediate) shell of the platelet, the one that contains the hydrophobic domain of P80 molecules embedded in the CP region (represented in cyan in Fig. 3 panel B), we can write

$$\sum_{f=2}^{3} \sum_{j=2}^{5-f} <V_{f,j}> = 2\pi(t_0 + t_2)(R_0^2(1 + \xi_R^2) + 2t_2 R_0 + t_2^2) - 2\pi t_0 R_0^2(1 + \xi_R^2)$$
$$= <N_{P80,pl}> (\nu_{P80,hyd} + \hat{r}_{CP,P80} \bar{\nu}_{CP}) \tag{S107}$$

where $\hat{r}_{CP,P80}$ represents the average number of CP molecules *per* P80 molecule in the second platelet shell. This definition allows to calculate the average molecular volume of CP in the whole platelet,

$$\bar{\nu}_{CP} = \bar{\nu}_{CP,3} + \frac{y_{P80} \hat{r}_{CP,P80}}{r_{CP,P80} k_{r_{CP,P80}}} (\nu_{CP,\alpha} - \bar{\nu}_{CP,3}) \tag{S108}$$

where we have assumed that in the second platelet's shell, all CP molecules are in the amorphous configuration. Combining Eqs. S103-S108 it is easy to analytically find out $\hat{r}_{CP,P80}$ as well as $<N_{CP,pl}>$, $<N_{P80,pl}>$ and $\bar{\nu}_{CP}$. We can also calculate both the overall volume fraction of CP and

the volume fraction of CP in the inner part of the platelets, according to,

$$\phi_{\text{CP}} = \frac{N_A c_{\text{CP}} \bar{\nu}_{\text{CP}}}{M_{\text{CP}}} \tag{S109}$$

$$\phi_{\text{CP},3} = \phi_{\text{CP}} \left( 1 - \frac{y_{\text{P80}} \hat{r}_{\text{CP,P80}} \nu_{\text{CP},\alpha}}{\bar{\nu}_{\text{CP}} r_{\text{CP,P80}} k_{r_{\text{CP,P80}}}} \right) \tag{S110}$$

The average area of the platelet associated with each P80 molecule can be calculated by referring to the second layer of the platelet and considering the ratio between the sum of the volume occupied by the hydrophobic domain of P80 and the one occupied by $\hat{r}_{\text{CP,P80}}$ molecules of CP and the thickness of this layer,

$$a_{\text{P80,pl}} = \frac{\nu_{\text{P80,hyd}} + \hat{r}_{\text{CP,P80}} \nu_{\text{CP},\alpha}}{t_2} \tag{S111}$$

To note, by assuming an average hexagonal displacement of the P80 molecules on the platelet surface, the average distance between the nearest neighbor P80 molecules is

$$d_{\text{P80,P80}} = \sqrt{2 a_{\text{P80,pl}} / \sqrt{3}} \tag{S112}$$

We also consider the number of water molecules associated with each P80 molecule occupying the first layer region of the platelet (shown in green in Fig. 3), indicated with $r_{\text{wat,P80}}$. On the other hand, the thickness of the first layer of the platelet can be calculated by taking into account the volume occupied by the polar head of P80 and the one due to $r_{\text{wat,P80}}$ water molecules, supposed to have a relative mass density $\hat{d}_{\text{wat,pl}}$ in respect to the bulk water mass density

$$t_1 = \frac{\nu_{\text{P80,pol,dry}} + r_{\text{wat,P80}} \frac{\nu_{\text{wat}}^{\circ}}{\hat{d}_{\text{wat,pl}} d_{\text{wat}}}}{a_{\text{P80,pl}}} \tag{S113}$$

Therefore, we can calculate the fraction of the platelet surface occupied by the polar head of P80

$$\phi_{S,\text{P80}} = \frac{\nu_{\text{P80,pol,dry}}}{t_1 a_{\text{P80,pl}}} \tag{S114}$$

The electron density of the 1-domain of the platelet results,

$$\rho_{f,1} = (e_C + 2e_O + 29e_{CH_2} + 2e_{CH_3} + r_{wat,P80}e_{H_2O})$$

$$/(\nu_{P80,pol,dry} + r_{wat,P80}\frac{\nu_{wat}^\circ}{\hat{d}_{wat,pl}d_{wat}}) \tag{S115}$$

The electron density of the 2-domain of the platelet results,

$$\rho_{f,2} = (14e_{CH_2} + 2e_{CH} + e_{CH_3} + \hat{r}_{CP,P80}(e_C + 2e_O + 29e_{CH_2} + 2e_{CH_3}))$$

$$/(\nu_{P80,hyd} + \hat{r}_{CP,P80}\bar{\nu}_{CP}) \tag{S116}$$

Finally, the third ED values correspond to the average electron density of the CP molecule, given in Eq. S94.

$$\rho_{f,3} = \rho_{CP,0} \tag{S117}$$

### S11.3.3 Barrels with shells

The average volume of the region between two subsequent platelets (represented in white in Fig. 3 panel B) is

$$V_0 = 2\pi\Delta t[R_0^2(1 + \xi_R^2) + t_2^2 + t_1^2 + 2R_0(t_2 + t_1) + 2t_2t_1] \tag{S118}$$

The average volume of the first shell region of platelets (represented in green in Fig. 3 panel B) is

$$V_1 = = 2\pi t_1[R_0^2(1 + \xi_R^2) + t_2(2R_0 + t_2) + (t_0 + t_2 + t_1)(2R_0 + 2t_2 + t_1)] \tag{S119}$$

The average volume of the second shell region of platelets (represented in cyan in Fig. 3 panel B) is

$$V_2 = 2\pi t_2[R_0^2(1 + \xi_R^2) + (t_0 + t_2)(2R_0 + t_2)] \tag{S120}$$

The average volume of the core region of platelets (represented in blue in Fig. 3 panel B) is

$$V_3 = 2\pi t_0 R_0^2(1 + \xi_R^2) \tag{S121}$$

S30

The average ED of barrels is

$$\rho_{\text{brl}} = \frac{\rho_{\text{wat}}V_0 + \rho_{f,1}V_1 + \rho_{f,2}V_2 + \rho_{f,3}V_3}{V_0 + V_1 + V_2 + V_3} \tag{S122}$$

The average number density of barrels is

$$\begin{aligned}
n_{\text{brl}} &= \frac{N_A c_{\text{CP}}}{M_{\text{CP}} <N_{\text{CP,pl}}> N_c} \\
&= \frac{\phi_{\text{CP}}}{\bar{\nu}_{\text{CP}} <N_{\text{CP,pl}}> N_c} \tag{S123}
\end{aligned}$$

The volume fractions of CP, P80 and water in the barrel are

$$\phi_{\text{brl,CP}} = \frac{<N_{\text{CP,pl}}> \bar{\nu}_{\text{CP}}}{D} \tag{S124}$$

$$\phi_{\text{brl,P80}} = \frac{<N_{\text{P80,pl}}> (\nu_{\text{P80,hyd}} + \nu_{\text{P80,pol,dry}})}{D} \tag{S125}$$

$$\phi_{\text{brl,wat}} = \frac{(<N_{\text{P80,pl}}> r_{\text{wat,P80}}/\hat{d}_{\text{wat,pl}} + V_0)\nu^\circ_{\text{wat}}/d_{\text{wat}}}{D} \tag{S126}$$

where

$$\begin{aligned}
D &= (<N_{\text{P80,pl}}> r_{\text{wat,P80}}/\hat{d}_{\text{wat,pl}} + V_0)\nu^\circ_{\text{wat}}/d_{\text{wat}} \\
&\quad + <N_{\text{P80,pl}}> (\nu_{\text{P80,hyd}} + \nu_{\text{P80,pol,dry}}) + <N_{\text{CP,pl}}> \bar{\nu}_{\text{CP}} \tag{S127}
\end{aligned}$$

### S11.3.4 Average surface of the barrel

The surface of a barrel with height $H$, major and minor radii $\nu R_M$ and $R_M$, respectively, results

$$S_{\text{brl}} = 2\pi R_M^2(\nu + 2)f(\varepsilon, \nu) \tag{S128}$$

where $\varepsilon = 2R_M/H$ and the function $f(\varepsilon, \nu)$, corresponds to the following integral

$$f(\varepsilon, \nu) = \frac{1}{\varepsilon} \int_0^1 \left[\nu + (1 - \nu)\sqrt{1 - \phi^2}\right] \sqrt{1 + \frac{\varepsilon^2 \phi^2 (1 - \nu)^2}{1 - \phi^2}} d\phi \tag{S129}$$

that can be easily derived in the framework of the revolution solid theory. We have solved numerically the integral in Eq. S129 in a two-dimensional grid of $\varepsilon$ and $\nu$ in the corresponding ranges $\frac{1}{5} \leq \varepsilon \leq 5$ and $0 \leq \nu \leq 1$. Subsequently, we have expanded the results in power series of $\nu$ up to

| $j$ | $b_{0,j}$ | $b_{1,j}$ | $c_{1,j}$ | $b_{2,j}$ | $c_{2,j}$ | $b_{3,j}$ | $c_{3,j}$ |
|---|---|---|---|---|---|---|---|
| 0 | 0.5382 | -0.0739 | 0.1724 | -2.9555 | 6.0253 | 1.3475 | 2.3820 |
| 1 | 0.8831 | 0.3803 | -0.6286 | 2.3728 | -9.8397 | -8.1622 | -3.6075 |
| 2 | -0.8858 | -0.6223 | -0.2495 | -0.2482 | -0.3393 | -0.0033 | -0.3686 |
| 3 | 11.0761 | 2.8980 | 0.2566 | -0.5802 | 1.1276 | -1.1853 | 0.4495 |
| 4 | -12.0772 | -11.3033 | -5.5527 | -4.6906 | -5.6968 | -4.7512 | -6.1686 |
| 5 | 3.5727 | 0.9426 | 0.2049 | 1.0701 | 3.0945 | 7.7301 | 0.9234 |
| 6 | -3.6432 | -3.0487 | -1.2873 | -0.2511 | -0.5396 | -0.2639 | -0.5900 |

Table S1: Expansion coefficients according to Eqs. S130 and S131.

the $6^{\text{th}}$ degree

$$f(\varepsilon, \nu) \approx \sum_{j=0}^{6} a_j(\varepsilon)\nu^j \tag{S130}$$

We have then approximated the coefficients $a_j(\varepsilon)$ with a combination of three exponential functions over a background,

$$a_j(\varepsilon) = b_{0,j} + \sum_{k=1}^{3} b_{k,j} e^{c_{k,j}\varepsilon} \tag{S131}$$

Best fitting parameters are shown in Table S1 The comparison between the integrals and their approximations due to Eqs. S130 and S131 is shown in Fig. S6. The double expansion allows an analytical calculation of the mean barrel surface, according to Gaussian distributions of both $R_M$ and $e$,

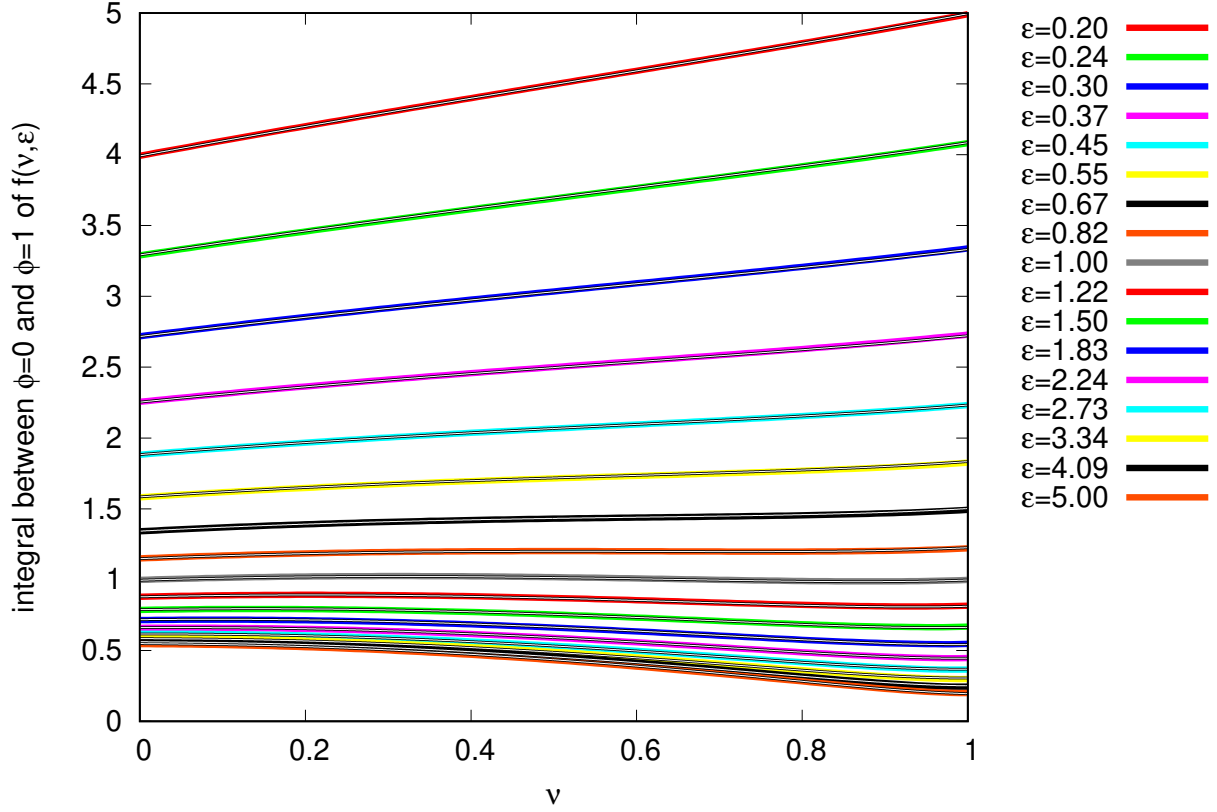$$<S_{\text{brl}}> = 2\pi <R_M^2>_{R_M} (\nu + 2) <f(\varepsilon, \nu)>_\varepsilon . \tag{S132}$$

Figure S6: Best fit of the integral expressed in Eq. S129 according to Eqs. S130 and S131.

The first average is given by

$$
\begin{aligned}
<R_M^2>_{R_M} &= \frac{1}{Z_{R_M}} \int_{R_{M,\mathrm{lb}}}^{R_{M,\mathrm{ub}}} R_M^2 e^{-(R_M - R_{M,\max})^2/(2\xi_{R_M}^2 R_{M,\max}^2)} \\
&= \frac{G_3}{Z_{R_M}}
\end{aligned}
$$

$$
\begin{aligned}
G_3 &= \frac{\sqrt{\pi}\left(\sqrt{2}\xi_{R_M}^3 R_{M,\max}^3 + \sqrt{2}\xi_{R_M} R_{M,\max}^3\right) - 4\xi_{R_M}^2 R_{M,\max}^3}{2} \\
&+ \frac{4\xi_{R_M}^2 R_{M,\max}^3 + \sqrt{\pi}\left(\sqrt{2}\xi_{R_M}^3 R_{M,\max}^3 + \sqrt{2}\xi_{R_M} R_{M,\max}^3\right)}{2} \\
&- e^{-\frac{1}{2\xi_{R_M}^2} - \frac{R_{M,\mathrm{lb}}^2}{2\xi_{R_M}^2 R_{M,\max}^2}}\left(\xi_{R_M}^2 R_{M,\max}^2\left(-2R_{M,\mathrm{lb}} - 2R_{M,\max}\right)e^{\frac{R_{M,\mathrm{lb}}}{\xi_{R_M}^2 R_{M,\max}}}\right. \\
&+ \sqrt{\pi}e^{\frac{1}{2\xi_{R_M}^2} + \frac{R_{M,\mathrm{lb}}^2}{2\xi_{R_M}^2 R_{M,\max}^2}}\left(\sqrt{2}\xi_{R_M}^3 R_{M,\max}^3 \mathrm{erfc}\left(\frac{\sqrt{2}R_{M,\max} - \sqrt{2}R_{M,\mathrm{lb}}}{2\xi_{R_M} R_{M,\max}}\right)\right. \\
&+ \left.\left.\sqrt{2}\xi_{R_M} R_{M,\max}^3 \mathrm{erfc}\left(\frac{\sqrt{2}R_{M,\max} - \sqrt{2}R_{M,\mathrm{lb}}}{2\xi_{R_M} R_{M,\max}}\right)\right)\right)/2 \\
&- e^{-\frac{1}{2\xi_{R_M}^2} - \frac{R_{M,\mathrm{ub}}^2}{2\xi_{R_M}^2 R_{M,\max}^2}}\left(\xi_{R_M}^2 R_{M,\max}^2\left(2R_{M,\mathrm{ub}} + 2R_{M,\max}\right)e^{\frac{R_{M,\mathrm{ub}}}{\xi_{R_M}^2 R_{M,\max}}}\right. \\
&+ \sqrt{\pi}e^{\frac{1}{2\xi_{R_M}^2} + \frac{R_{M,\mathrm{ub}}^2}{2\xi_{R_M}^2 R_{M,\max}^2}}\left(\sqrt{2}\xi_{R_M}^3 R_{M,\max}^3 \mathrm{erfc}\left(\frac{\sqrt{2}R_{M,\mathrm{ub}} - \sqrt{2}R_{M,\max}}{2\xi_{R_M} R_{M,\max}}\right)\right. \\
&+ \left.\left.\sqrt{2}\xi_{R_M} R_{M,\max}^3 \mathrm{erfc}\left(\frac{\sqrt{2}R_{M,\mathrm{ub}} - \sqrt{2}R_{M,\max}}{2\xi_{R_M} R_{M,\max}}\right)\right)\right)/2/\sqrt{2}
\end{aligned} \tag{S133}
$$

where $Z_{R_M}$ is calculated with Eq. S22. The second average depends on the mean value of $\varepsilon$, $\varepsilon_0 = 2R_{M,0}/H_0$, and its variance $\sigma_\varepsilon^2 = \varepsilon_0^2 \xi_{R_M}^2 + \varepsilon_0^4 \sigma_H^2/(4R_{M,0}^2)$ where $\sigma_H^2 = H_0^2 \sigma_{N_c}^2 + 4\xi_t^2 N_c^2 t_0^2$. To notice, $R_{M,0}$ is the average maximum circular cross-section radius of the barrel, according to

$$
\begin{aligned}
R_{M,0} &= \frac{1}{Z_{R_M}} \int_{R_{M,\mathrm{lb}}}^{R_{M,\mathrm{ub}}} R_M e^{-(R_M - R_{M,\mathrm{max}})^2/(2\xi_{R_M}^2 R_{M,\mathrm{max}}^2)} \\[2mm]
&= \frac{G_4}{Z_{R_M}} \\[2mm]
G_4 &= \sqrt{2\pi}\xi_{R_M} R_{M,\mathrm{max}}^2 \\[2mm]
&\quad -\frac{1}{2} e^{-\frac{1}{2\xi_{R_M}^2} - \frac{R_{M,\mathrm{lb}}^2}{2\xi_{R_M}^2 R_{M,\mathrm{max}}^2}} \left( \sqrt{2\pi}\xi_{R_M} R_{M,\mathrm{max}}^2 e^{\frac{1}{2\xi_{R_M}^2} + \frac{R_{M,\mathrm{lb}}^2}{2\xi_{R_M}^2 R_{M,\mathrm{max}}^2}} \right. \\[2mm]
&\quad \left. \mathrm{erfc}\left( \frac{\sqrt{2}R_{M,\mathrm{max}} - \sqrt{2}R_{M,\mathrm{lb}}}{2\xi_{R_M} R_{M,\mathrm{max}}} \right) - 2\xi_{R_M}^2 R_{M,\mathrm{max}}^2 e^{\frac{R_{M,\mathrm{lb}}}{\xi_{R_M}^2 R_{M,\mathrm{max}}}} \right) \\[2mm]
&\quad -\frac{1}{2} e^{-\frac{1}{2\xi_{R_M}^2} - \frac{R_{M,\mathrm{ub}}^2}{2\xi_{R_M}^2 R_{M,\mathrm{max}}^2}} \left( 2\xi_{R_M}^2 R_{M,\mathrm{max}}^2 e^{\frac{R_{M,\mathrm{ub}}}{\xi_{R_M}^2 R_{M,\mathrm{max}}}} + \sqrt{2\pi}\xi_{R_M} R_{M,\mathrm{max}}^2 e^{\frac{1}{2\xi_{R_M}^2} + \frac{R_{M,\mathrm{ub}}^2}{2\xi_{R_M}^2 R_{M,\mathrm{max}}^2}} \right. \\[2mm]
&\quad \left. \mathrm{erfc}\left( \frac{\sqrt{2}R_{M,\mathrm{ub}} - \sqrt{2}R_{M,\mathrm{max}}}{2\xi_{R_M} R_{M,\mathrm{max}}} \right) \right)
\end{aligned}
\tag{S134}
$$

As a result, we have obtained the following analytical expression for the average $<f(\varepsilon,\nu)>_\varepsilon$

$$
\begin{aligned}
<f(\varepsilon,\nu)>_\varepsilon &\approx \sum_{j=0}^{6} <a_j(\varepsilon)>_\varepsilon \nu^j \\[2mm]
<a_j(\varepsilon)>_\varepsilon &= \frac{1}{Z_\varepsilon} \int_{\varepsilon_{\mathrm{lb}}}^{\varepsilon_{\mathrm{ub}}} a_j(\varepsilon) e^{-(\varepsilon-\varepsilon_0)^2/(2\sigma_\varepsilon^2)} d\varepsilon \\[2mm]
&= b_{0,j} + \frac{1}{2Z_\varepsilon} \sum_{k=1}^{3} b_{k,j} e^{c_{k,j}(\varepsilon_0 + c_{k,j}\sigma_\varepsilon^2/2)} \\[2mm]
&\quad \times \left[ \mathrm{erf}\left( \frac{\varepsilon_0 - \varepsilon_{\mathrm{lb}} + c_{k,j}\sigma_\varepsilon^2}{\sqrt{2}\sigma_\varepsilon} \right) - \mathrm{erf}\left( \frac{\varepsilon_0 - \varepsilon_{\mathrm{ub}} + c_{k,j}\sigma_\varepsilon^2}{\sqrt{2}\sigma_\varepsilon} \right) \right] \\[2mm]
Z_\varepsilon &= \int_{\varepsilon_{\mathrm{lb}}}^{\varepsilon_{\mathrm{ub}}} e^{-(\varepsilon-\varepsilon_0)^2/(2\sigma_\varepsilon^2)} d\varepsilon \\[2mm]
&= \frac{1}{2} \left[ \mathrm{erf}\left( \frac{\varepsilon_{\mathrm{ub}} - \varepsilon_0}{\sqrt{2}\sigma_\varepsilon} \right) - \mathrm{erf}\left( \frac{\varepsilon_{\mathrm{lb}} - \varepsilon_0}{\sqrt{2}\sigma_\varepsilon} \right) \right]
\end{aligned}
$$

$$\tag{S135}$$
$$\tag{S136}$$

where the two integral bounds are $\varepsilon_{\mathrm{lb}} = \max\{1/5, \varepsilon_0 - p\sigma_\varepsilon\}$ and $\varepsilon_{\mathrm{ub}} = \min\{5, \varepsilon_0 + p\sigma_\varepsilon\}$.

## S12 SAXS amplitude of $N_s$ layers of electron densities with smooth transitions

The excess ED profile of $N_s$ layers with smooth transition in respect to the bulk water ED $\rho_0$ is

$$\delta\rho_{\text{brl}}(z) \;\; = \;\; \frac{1}{2}\sum_{j=0}^{N_s}(\rho_{j+1,\text{brl}} - \rho_{j,\text{brl}})\left[1 + \text{erf}\left(\frac{z - z_{j,\text{brl}}}{2^{1/2}\sigma_{j,\text{brl}}}\right)\right] \tag{S137}$$

where $z_{j,\text{brl}} = \sum_{k=1}^{j}\tau_{k,\text{brl}}$ is the $z$ coordinate of the plane that separates the $(j+1)$-layer (with ED $\rho_{j+1,\text{brl}}$) and the $j$-layer (with ED $\rho_{j,\text{brl}}$) with the assumption $z_{0,\text{brl}} = 0$, $\tau_{k,\text{brl}}$ is the thickness of the $k$-layer, $\sigma_{j,\text{brl}}$ is the smooth parameter between $(j+1)$-layer and the $j$-layer and with the assumption $\rho_{0,\text{brl}} \equiv \rho_0$. To note, in the case of $N_s = 0$, there is only a smooth transition between 0-layer (bulk) and 1-layer (overall barrel). The Fourier transform of Eq. S137 is

$$A_{\text{brl}}(q) \;\; = \;\; \frac{i}{q}\sum_{j=0}^{N_s}(\rho_{j+1,\text{brl}} - \rho_{j,\text{brl}})e^{-\frac{1}{2}(q\sigma_{j,\text{brl}})^2}e^{iqz_{j,\text{brl}}} \tag{S138}$$

To note, in the case $N_s = 0$ and for $\sigma_{0,\text{brl}} = 0$ we have $|A_{\text{brl}}(q)|^2 = q^{-2}(\rho_{1,\text{brl}} - \rho_0)^2$, which, combined with Eq. 20, leads to the typical $q^{-4}$ Porod behaviour.

| Time from preparation (days) | $<R_H>$ (Å) | $\xi_{R_H}$ |
|---|---|---|
| 0 | 939±6 | 0.29±0.02 |
| 2 | 988±8 | 0.32±0.02 |
| 6 | 963±7 | 0.31±0.02 |
| 15 | 938±9 | 0.29±0.02 |
| 30 | 959±5 | 0.28±0.01 |

Table S2: Mean hydrodynamic radius of the LNS and associated dispersion obtained from the analysis of the second-order autocorrelation functions measured by DLS.

Table S3: Common fitting parameters obtained by the analysis of SAXS curves as recorded at the Austrian SAXS beamline at ELETTRA. The unit of length is Å. Validity ranges of fitting parameters: [a] $[-1000, 1000]$ (kJ/mol); [b] $[-50, 50]$ (kJ/mol); [c] $[12.0, 15.0]$; [d] $[11.0, 14.0]$; [e] $[14.0, 17.0]$; [f] $[14.0, 17.0]$; [g] $[19.8, 23.0]$; [h] $[26.2, 27.5]$; [i] $[48.0, 54.0]$; [j] $[29.8, 30.0]$; [k] $[0.95, 1.00]$; [l] $[0.95, 1.00]$; [m] $[7.1, 7.8]$ $(10^{-4}$ K$^{-1})$; [n] $[0.97, 1.15]$; [o] $[0.97, 1.15]$; [p] $[0.97, 1.15]$

| | | |
|---|---|---|
| $\Delta$ | [a] | $-348 \pm 3$ |
| $\delta$ | [b] | $-24.7 \pm 0.2$ |
| $\nu^{\circ}_{>C=}$ | [c] | $13.0 \pm 0.1$ |
| $\nu^{\circ}_{=O}$ | [d] | $12.0 \pm 0.1$ |
| $\nu^{\circ}_{-O-}$ | [e] | $15.5 \pm 0.2$ |
| $\nu^{\circ}_{OH}$ | [f] | $14.0 \pm 0.1$ |
| $\nu^{\circ}_{CH}$ | [g] | $20.4 \pm 0.2$ |
| $\nu^{\circ}_{CH_2}$ | [h] | $26.5 \pm 0.3$ |
| $\nu^{\circ}_{CH_3}$ | [i] | $50.1 \pm 0.5$ |
| $\nu^{\circ}_{H_2O}$ | [j] | $29.8 \pm 0.3$ |
| $\beta_{CH_2}$ | [k] | $0.97 \pm 0.01$ |
| $\beta_{CH_3}$ | [l] | $0.97 \pm 0.01$ |
| $\alpha_{lip}$ | [m] | $7.22 \pm 0.07$ |
| $\hat{d}_{wat,cyl}$ | [n] | $1.12 \pm 0.01$ |
| $\hat{d}_{wat,cap}$ | [o] | $1.01 \pm 0.01$ |
| $\hat{d}_{wat,pl}$ | [p] | $0.99 \pm 0.01$ |

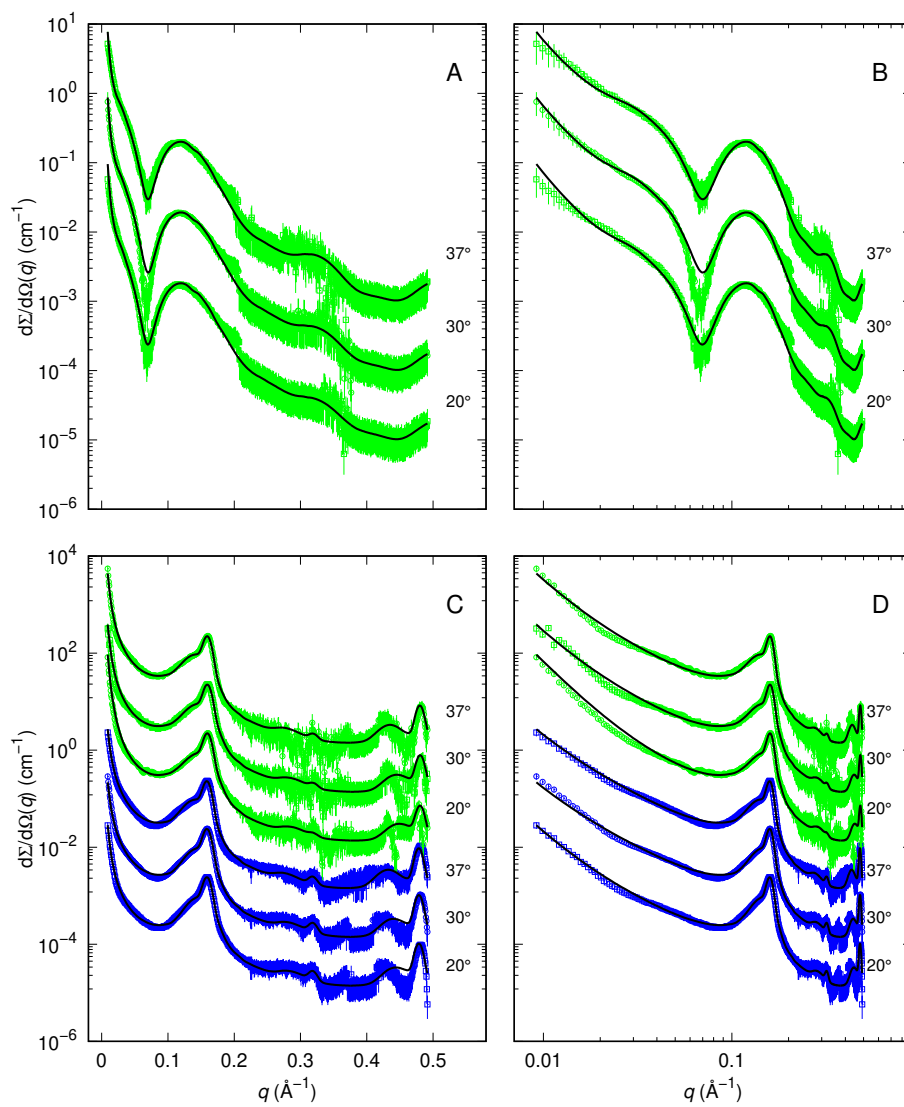## S13 SAXS analysis of the data recorded at ELETTRA

Figure S7: Synchrotron SAXS curves recorded the Austrian SAXS beamline of ELETTRA of P80 (panels A-B) and LNP (panels C-D) samples reported in semi-logarithmic plot (panels A, C) and in logarithmic plots (panels B and D), respectively. For a better visualization, curves have been stacked by multiplying for a factor $10^{m-1}$, $m$ being the index of the row from the bottom. In panels A-B, data refer to 13.3 g/L P80 concentration. Green and blue points in panels C-D refer to 80.0 and 40.0 g/L LNP concentration, respectively. Solid black lines are the best fits obtained with the global-fit method.
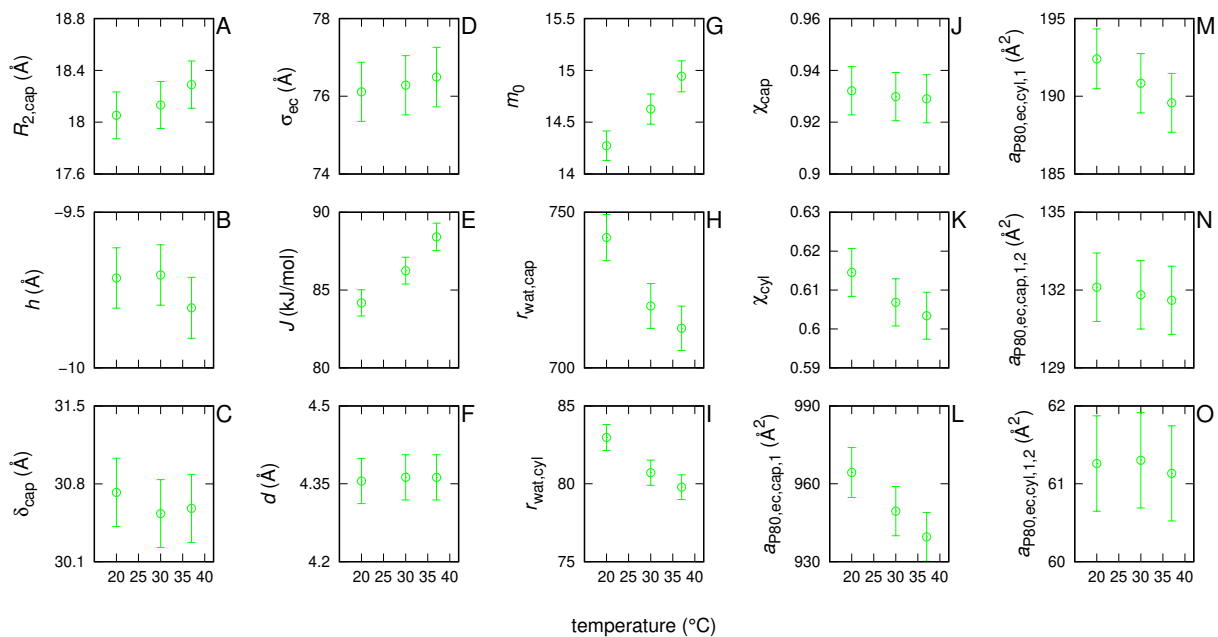
Figure S8: Second-class fitting parameters (panels A-F) and derived fitting parameters (panels G-O) obtained by the analysis of SAXS data recorded at the Austrian SAXS beamline at ELETTRA of P80 shown in Fig. S7 (panels A-B). Points refer to 13.3 g/L P80 concentration. The validity ranges of the fit parameters shown in the panels are: A) [6,30] Å; B) [-30,30] Å; C) [6,50] Å; D) [0,100] Å; E) [0,500] kJ/mol; F) [0.1,10] Å.
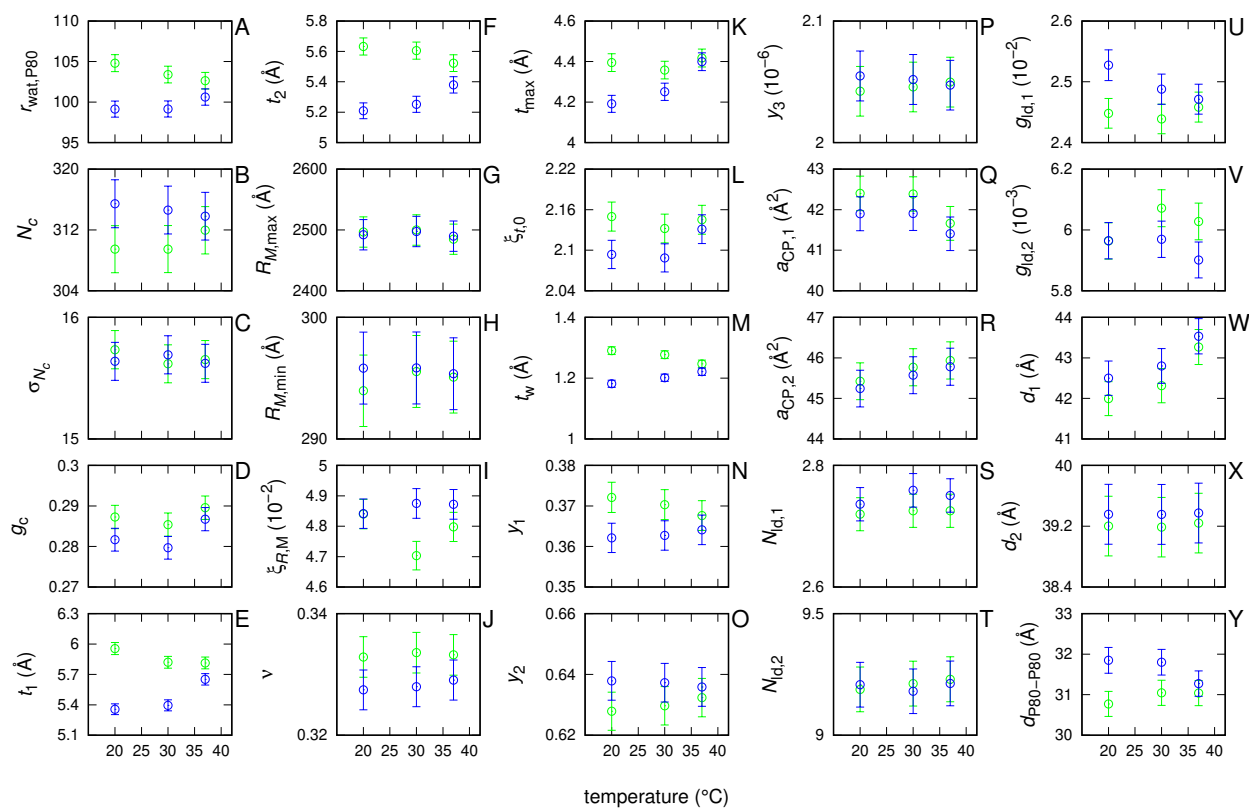
Figure S9: Second-class fitting parameters (panels A, B, C, D, F, G, H, I, J, K, L, M, N, O, Q, R, S, T, U, V) and derived fitting parameters (panels E, P, W, X, Y) obtained by analyzing SAXS data recorded at the Austrian SAXS beamline at ELETTRA of LNP shown in Fig. 3 (panels C-D). Green and blue points refer to 80.0 and 40.0 g/L LNP concentration, respectively. The validity ranges of the fit parameters shown in the panels are: A) [35,500]; B) [10,500]; C) [2,100]; D) [0,2]; F) [4,20] Å; G) [600,3000] Å; H) [100,400] Å; I) [0,5]; J) [0,1]; K) [3,40] Å; L) [0,10]; M) [0,30] Å; N) [0,1]; O) [0,1]; Q) [30,65] $Å^2$; R) [30,65] $Å^2$; S) [1,20]; T) [1,20]; U) [0,1]; V) [0,1].
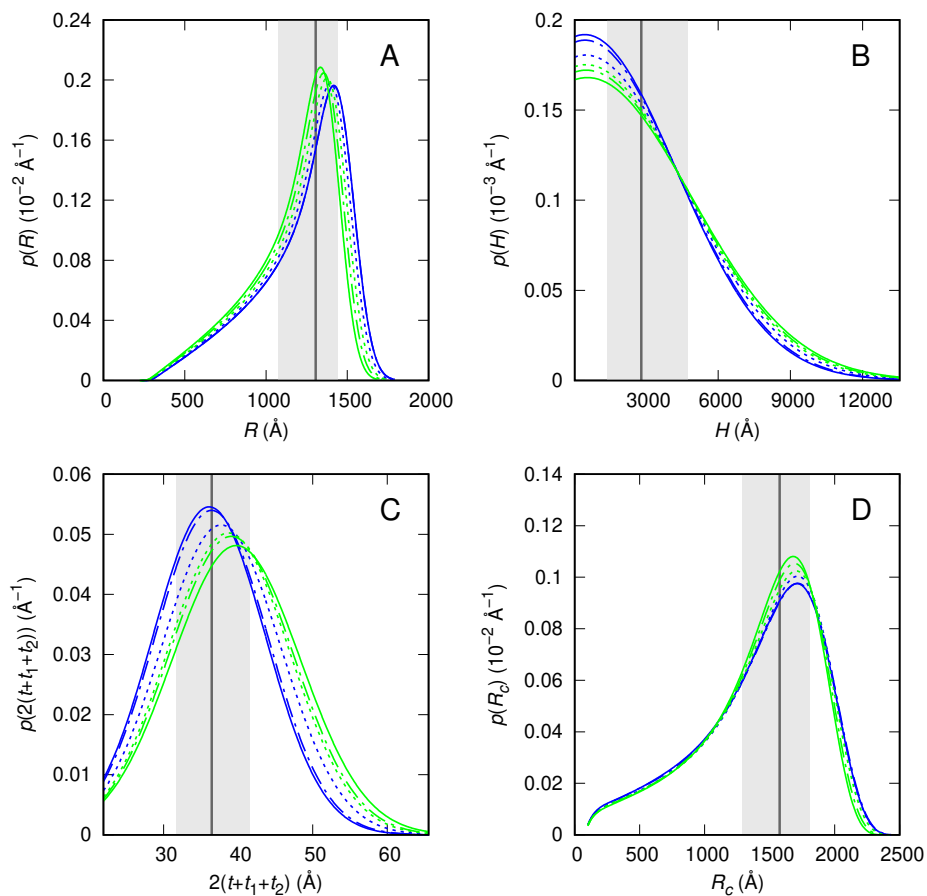
Figure S10: Probability densities of the circular cross-section barrel radius (panel A), of the total thickness of the platelets (panel B), of the barrel height (panel C) and of the center-to-border distance (panel D) obtained by the analysis of SAXS data recorded at the Austrian SAXS beamline of ELETTRA. Green and blue lines refer to 80.0 and 40.0 g/L LNP concentration. Solid, dotted, and dashed lines refer to the temperature of 20, 25, and 37 °C. In all panels, the dark-gray vertical lines indicate the median at 80.0 g/L and 20 °C, and the shaded area indicates the corresponding range between 1st and 3rd quartile.
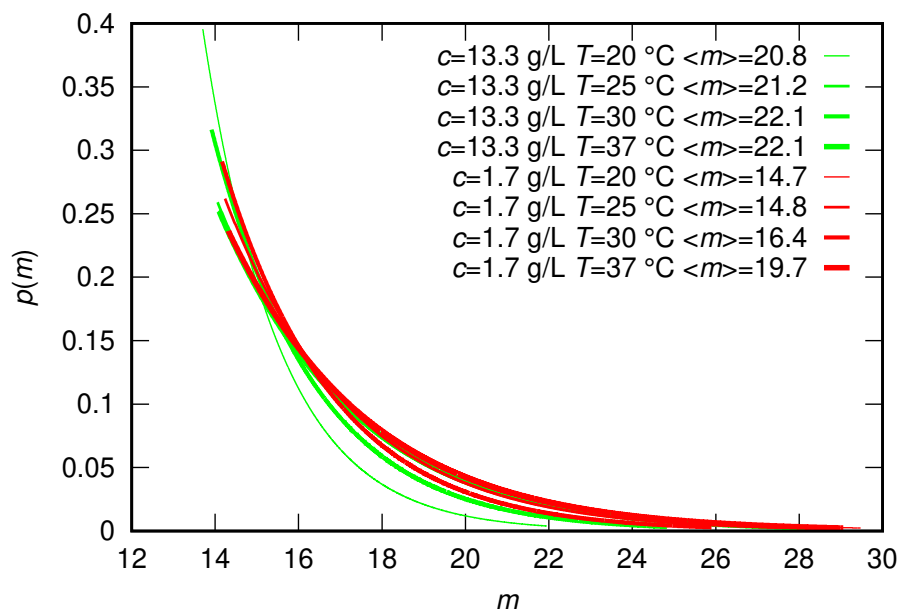
Figure S11: Size distribution of a cylinder with spherical end-caps micelle resulting from the fit of SAXS data recorded at the ID02 beamline at ESRF on P80 samples.
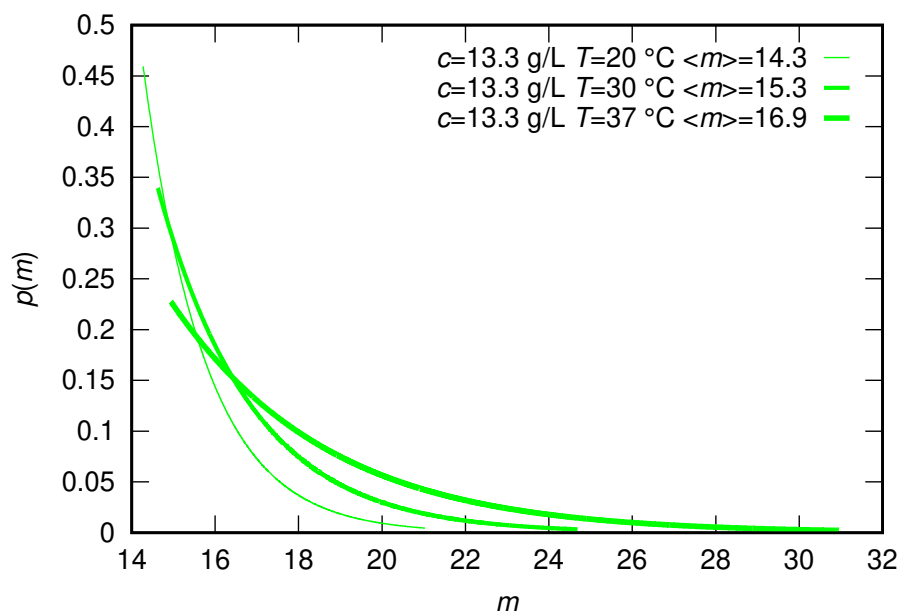


Figure S12: Size distribution of a cylinder with spherical end-caps micelle resulting from the fit of SAXS data recorded at the Austrian SAXS beamline of ELETTRA on P80 samples.
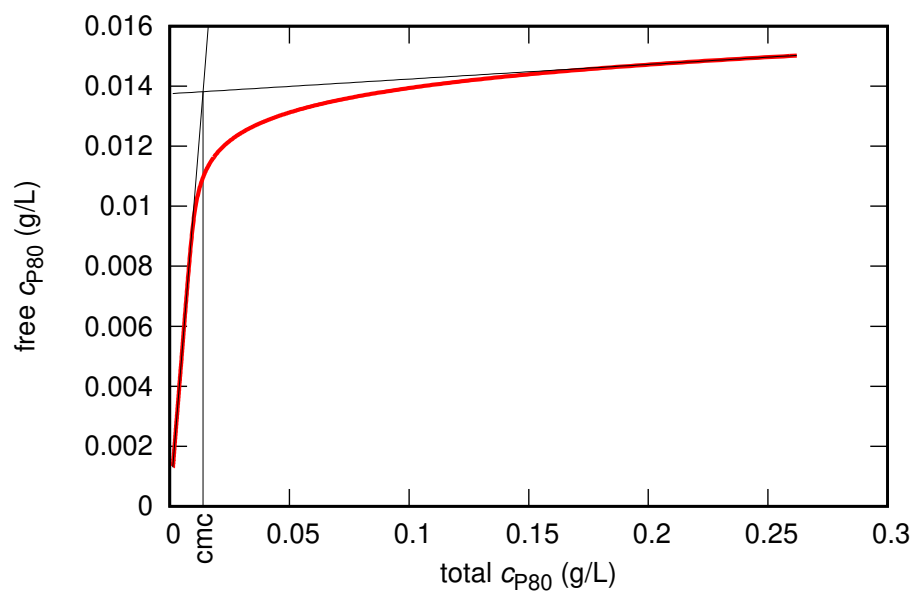
Figure S13: Concentration of free P80 molecules in solution as a function of the total concentration of the molecules calculated on the basis of the fitting parameters of SAXS curves. Linear fittings at the beginning and the end of the curve allow us to calculate the cmc of P80.

# References

[1] Kaya, H. Scattering from cylinders with globular end-caps. *Journal of Applied Crystallography* **2004**, *37*, 223–230.

[2] Spinozzi, F.; Paccamiccio, L.; Mariani, P.; Amaral, L. Q. Melting Regime of the Anionic Phospholipid DMPG: New Lamellar Phase and Porous Bilayer Model. *Langmuir* **2010**, *26*, 6484–6493.

[3] De Rosa, R.; Spinozzi, F.; Itri, R. Hydroperoxide and carboxyl groups preferential location in oxidized biomembranes experimentally determined by small angle X-ray scattering: Implications in membrane structure. *BBA - Biomembranes* **2018**, *1860*, 2299–2307.

[4] Maxima, Maxima, a Computer Algebra System. Version 5.46.0. **2022**,

[5] Spinozzi, F.; Ortore, M. G.; Nava, G.; Bomboi, F.; Carducci, F.; Amenitsch, H.; Bellini, T.; Sciortino, F.; Mariani, P. Gelling without Structuring: A SAXS Study of the Interactions among DNA Nanostars. *Langmuir* **2020**, *36*, 10387–10396.